AFRL-SN-RS-TR-2000-30 Vol II (of two)
Final Technical Report
March 2001

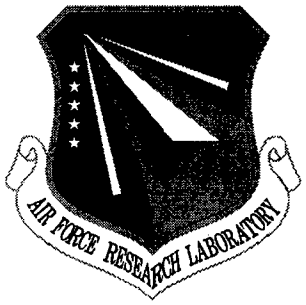


# INCREASING SECONDARY DATA OR ENHANCED ADAPTIVE DISPLACED PHASE CENTERED ANTENNA APPROACHES

**Capraro Technologies, Inc.**

**Gerard T. Capraro, Christopher T. Capraro, and Donald D. Weiner**

*APPROVED FOR PUBLIC RELEASE; DISTRIBUTION UNLIMITED.*



**AIR FORCE RESEARCH LABORATORY**
**SENSORS DIRECTORATE**
**ROME RESEARCH SITE**
**ROME, NEW YORK**

Although this report references (*) limited report on page 49, no limited information has been extracted.

This report has been reviewed by the Air Force Research Laboratory, Information Directorate, Public Affairs Office (IFOIPA) and is releasable to the National Technical Information Service (NTIS). At NTIS it will be releasable to the general public, including foreign nations.

AFRL-SN-RS-TR-2001-30 Vol II (of two) has been reviewed and is approved for publication.

APPROVED:

DAVID B. BUNKER
Project Engineer

FOR THE DIRECTOR:

ROBERT G. POLCE, Chief
Rome Operations Office
Sensors Directorate

If your address has changed or if you wish to be removed from the Air Force Research Laboratory Rome Research Site mailing list, or if the addressee is no longer employed by your organization, please notify AFRL/SNRT, 26 Electronic Pky, Rome, NY 13441-4514. This will assist us in maintaining a current mailing list.

Do not return copies of this report unless contractual obligations or notices on a specific document require that it be returned.

| REPORT DOCUMENTATION PAGE | | | Form Approved OMB No. 0704-0188 |
|---|---|---|---|



| 1. AGENCY USE ONLY *(Leave blank)* | 2. REPORT DATE | 3. REPORT TYPE AND DATES COVERED |
|---|---|---|
| | MARCH 2001 | Final Mar 97 - Feb 98 |

**4. TITLE AND SUBTITLE**
INCREASING SECONDARY DATA OR ENHANCED ADAPTIVE DISPLACED PHASE CENTERED ANTENNA APPROACHES

**5. FUNDING NUMBERS**
C - F30602-97-C-0065
PE - 62702F
PR - 4506
TA - 11
WU - PJ

**6. AUTHOR(S)**
Gerard T. Capraro, Christopher T. Capraro, and Donald D. Weiner

**7. PERFORMING ORGANIZATION NAME(S) AND ADDRESS(ES)**
Prime: Capraro Technologies, Inc.
311 Turner Street - Suite 410
Utica NY 13501

Sub: Syracuse University
Dept. of Electrical
& Computer Engineering
Syracuse NY 13244

**8. PERFORMING ORGANIZATION REPORT NUMBER**
N/A

**9. SPONSORING/MONITORING AGENCY NAME(S) AND ADDRESS(ES)**
Air Force Research Laboratory/SNRT
26 Electronic Pky
Rome NY 13441-4514

**10. SPONSORING/MONITORING AGENCY REPORT NUMBER**
AFRL-SN-RS-TR-2001-30
Vol II (of two)

**11. SUPPLEMENTARY NOTES**
Air Force Research Laboratory Project Engineer: David B. Bunker/SNRT/(315) 330-2345

**12a. DISTRIBUTION AVAILABILITY STATEMENT**
APPROVED FOR PUBLIC RELEASE; DISTRIBUTION UNLIMITED.

**12b. DISTRIBUTION CODE**

**13. ABSTRACT** *(Maximum 200 words)*
A study of space-time adaptive processing in nonhomogeneous environments is presented. The results produced are logically organized as investigations into three different but related topics. The first topic can be summarized as an investigation of the performance of partially adaptive space-time adaptive processing schemes using measured (MCARM) data. The second topic considers the development of a new set of space-time processing algorithms, which use prior knowledge to reduce the number of parameters, which need to be adapted. The new schemes were tested using MCARM data. The final topic provides analytical realistic cases where the reference or training data may have different statistics from the data in the cell under test. Such equations have not yet appeared in the literature and they are useful for understanding the performance of space-time adaptive processing (STAP) schemes when they are tested with MCARM data.

**14. SUBJECT TERMS**
Space Time Adaptive Processing (STAP), Adaptive Array Processing (ASAP), Estimation Using Mismatched Statistics, Airborne Radar Signal Processing

**15. NUMBER OF PAGES**
60

**16. PRICE CODE**

| 17. SECURITY CLASSIFICATION OF REPORT | 18. SECURITY CLASSIFICATION OF THIS PAGE | 19. SECURITY CLASSIFICATION OF ABSTRACT | 20. LIMITATION OF ABSTRACT |
|---|---|---|---|
| UNCLASSIFIED | UNCLASSIFIED | UNCLASSIFIED | UL |

Standard Form 298 (Rev. 2-89) (EG)
Prescribed by ANSI Std. 239.18
Designed using Perform Pro, WHS/DIOR, Oct 94

## Table of Contents

## List of Figures

## List of Tables

# 1. INTRODUCTION

In this chapter, some partially adaptive space-time processing (PSTAP) schemes [1] are compared according to the performance obtained using a measured radar data set called multi-channel airborne measurements (MCARM). Algorithms studied include adaptive displaced phase centered antenna (ADPCA), factored post Doppler (FTS), extended factored approach (EFA), joint-domain localized (JDL), subarraying ADPCA, subarraying EFA, subarraying FTS, and beamspace ADPCA. We use normalized test statistics which achieve constant false alarm probability in homogenous clutter. The performance of the algorithms is studied in section 2.

## 1.1 Subarraying ADPCA

Let **N** be the number of antenna elements, **M** be the number of pulses per coherent processing interval (CPI), $\mathbf{K_s}$ be the number of beams formed and, $\mathbf{K_t}$ be the number of pulses which will be adaptively processed.

First the pre-processing performs the beamforming and forms groups of $\mathbf{K_t}$ pulses from $\mathbf{K_s}$ beam outputs as

$$\tilde{\mathbf{X}}_k(\mathbf{p}) = \left(\mathbf{A_p} \otimes \mathbf{G}\right)^H \mathbf{X_k} \quad ; \quad \mathbf{p = 0,1,2,....,P-1} \tag{1}$$

where $\mathbf{X_k}$ is the space-time snapshot organized as

$$\mathbf{X_k} = \left[\mathbf{x_{1,1,k}}, \mathbf{x_{2,1,k}}, \cdots, \mathbf{x_{N,1,k}}, \mathbf{x_{1,2,k}}, \cdots \mathbf{x_{N,M,k}}\right]^T \tag{2}$$

where $\mathbf{x_{i,j,k}}$ is the observation from the $i^{th}$ antenna element, $j^{th}$ pluse and $k^{th}$ range cell [2], **G** is the $\mathbf{N \times K_s}$ beamformer matrix , and

$$\mathbf{A_p} = \begin{bmatrix} \mathbf{0}_{p \times K_t} \\ \mathbf{I}_{K_t} \\ \mathbf{0}_{(M-K_t-p) \times K_t} \end{bmatrix} \tag{3}$$

where the notation $0_{q\times m}$ refers to an $q\times m$ matrix of zeros and $I_{Kt}$ is a $K_t\times K_t$ identity matrix. It is possible to form sub-CPIs which overlap by any number of pulses as in [2]. In this report we focus on the case where $K_t$ is set to 3 and consecutive sub-CPIs overlap two pulses. We also focus on $K_s=3$ in this report.

The beamformer matrix mentioned in [1] (See equation (256) on page 14 in [1].) is used in our processing. This matrix is

$$\mathbf{G} = \begin{bmatrix} g_0 & 0 & & 0 \\ g_1 & g_0 & & \\ \vdots & g_1 & \ddots & \\ g_{N'-1} & \vdots & & g_0 \\ & g_{N'-1} & \ddots & g_1 \\ & & & \vdots \\ 0 & 0 & & g_{N'-1} \end{bmatrix} \tag{4}$$

where $\mathbf{g} = (g_0, g_1, g_2, \ldots, g_{N'-1})^T$ is a vector of scalar components and $N'= N-K_s+1$ . The vector $\mathbf{g}$ could be defined as any of the popular windows or tapering from the DSP [3] or radar [4] literature. Here we take $\mathbf{g}$ as either a uniform window (all ones) or the hamming window in our tests. The uniform window gave better results than the hamming window so we present results for the uniform window. The $\mathbf{G}$ matrix in (4) represents a case where the beams use identical beamforming using a length $N'$ element subaperture, with each subaperture shifted by one element from the previous one. The resulting processing is sometimes called subarraying.

Each vector produced by the pre-processing (1) will be adaptively processed as

$$\mathbf{y}_k(p) = \mathbf{S}^H\mathbf{R}_k^{-1}(p)\tilde{\mathbf{X}}_k(p)/\Phi \tag{5}$$

where

$$\mathbf{S} = (\mathbf{I}_{Kt}\otimes\mathbf{G})^H\mathbf{S}_e \tag{6}$$

with $\mathbf{S}_e$ as

$$\mathbf{S}_e = \mathbf{S}_t\otimes\mathbf{S}_s \tag{7}$$

where $S_s$ is the $N\times1$ spatial target vector [1] and $S_t$ is a $K_t\times1$ vector of binomial coefficients of altering sign normally used in ADPCA [2]. The term $\Phi$ in the denominator of (5) is the normalization to provide CFAR in homogeneous clutter and is given by

$$\Phi = S^H R_k^{-1} S \tag{8}$$

$R_k$ is the interference-plus-noise covariance matrix estimated from the pre-processed data from the Q adjacent range cells (reference data), excluding the cell- under-test and the two closest cells on each side of the cell-under-test, as follows

$$R_k(p) = \frac{1}{Q} \sum_{i=k-Q/2-2, i\neq k-2,k-1,k,k+1,k+2}^{k+Q/2+2} \tilde{X}_i(p)\tilde{X}_i(p)H \tag{9}$$

After the adaptive processing, post processing is performed which can be expressed as

$$\tilde{Y}_k = \left[ y_k(0), y_k(1), \ldots, y_k(P-1) \right]^T \tag{10}$$

$$\tilde{Z}_{k,m} = f_m^H \tilde{Y}_k \tag{11}$$

assuming the target is in the $m^{th}$ Doppler bin. In this case $f_m$ is the $m^{th}$ column of a $P\times P$ Doppler filter matrix F, and $Z_{k,m}$ is the final output whose magnitude will be compared to a threshold to produce a decision. In the case of plain ADPCA (not subarraying) we set $G = I_N$.

## 1.2 Subarraying FTS (BFTS)

In subarraying factored post-Doppler (FTS) STAP, the pre-processing is described by (1) with $A_p = f_p$ and $P=M$. $f_p$ is the $p^{th}$ column of an $M\times M$ Doppler filter matrix $F=[f_0, f_1, f_2, \ldots, f_{M-1}]$. G is the $N\times K_s$ beamforming matrix as in subarraying ADPCA. This

pre-processing transforms the signal into Doppler space. To test for a target at a particular Doppler frequency, only one pre-processing from (1) needs to be calculated. In FTS a single pulse at a time is processed ($K_t$=1), and **p** indicates the Doppler bin in question. The adaptive processing in (5) is employed with the steering vector **S** defined as in (6) with $K_t$ =1. Here $S_e$ is set to $S_s$ in (7), since $K_t$ is 1. Post processing is not usually employed, so $|y_k(p)|$ is compared to a threshold to test for a target in the $p^{th}$ Doppler bin. In the case of plain FTS we set $G = I_N$.

## 1.3 Subarraying EFA (BEFA)

The subarraying extended factored approach (BEFA) is a slight extension of the subarraying FTS approach. In BEFA, adaptive processing is applied to several adjacent Doppler bins instead of just one. In our subarraying EFA implementation, the scheme adapts over 3 adjacent bins. The pre-processing is as in (1) with $A_p=[f_{p-1}, f_p, f_{p+1}]$. The pre-processing performs both transformation and selection. The adaptive processing is as in subarraying ADPCA with $S_t= [0\ 1\ 0]^T$. Post processing is not employed. In the case of plain EFA we set $G = I_N$.

## 1.4 Beamspace ADPCA (BeamAD)

In beamspace ADPCA , the pre-processing can be defined as in (1) with $A_p$ as in (3), and $G=[\ f_{N,1}, f_{N,2}, \ldots, f_{N,Ks}\ ]$, where $f_{N,j}$ $j=1, \ldots, K_s$ are the columns of N×N DFT matrix corresponding to $K_s$ angle bins. For simplicity assume $K_s$=3 and the target to be detected is in the $2^{nd}$ angle bin. The adaptive processing is as in subarraying ADPCA with $S=[0\ \ 1\ \ 0]\otimes S_t$, where $S_t$ is a $K_t \times 1$ vector of binomial coefficients of altering sign as in subarraying ADPCA. In our tests $K_s$ and $K_t$ were set to 3. The post processing is as in subarraying ADPCA as described by (10) and (11).

## 1.5 Joint-domaint localized approach (JDL)

In JDL, the pre-processor performs two dimensional transformation and selection. The data is transformed from the space-time domain into the angle-Doppler domain. This pre-processing can be described as in (1), with $A_p=[\ f_{m,1}, f_{m,2}, \ldots, f_{m,Kt}]$, where $f_{m,j}$ $j=1, \ldots\ldots, K_t$ are the columns of an M×M DFT matrix corresponding to the $K_t$ Doppler bins and with $G=[\ f_{n,1}, f_{n,2},$

..., $\mathbf{f}_{n,K_s}$ ], where $\mathbf{f}_{n,j}$ j=1, ..., $K_s$ are the columns of N×N DFT matrix corresponding to the $K_s$ angle bins. As for FTS and EFA only the post processing corresponding to a single **p** must be calculated to test for a target at a particular Doppler and Angular frequency.

If we again focus on $K_t = K_s = 3$ and consider the case where the target to be detected is in 2nd angle and the 2nd Doppler bin then, the adaptive processing can be described as in (5) with

$$\mathbf{S} = [0 \quad 1 \quad 0] \otimes [0 \quad 1 \quad 0] \tag{12}$$

More precisely, the steering vector has all its entries equal to zero except for the one corresponding to the angle and Doppler bin of the target. No post-processing is employed for JDL.

# 2. REAL DATA PERFORMANCE

To test the STAP algorithms described in section 1, we use data that comes from the MCARM database flight 5 acquisition 575. See [5] and [6] for detailed information about the MCARM program and the data. For each experiment, a single target signal with amplitude 0.05, a particular normalized Doppler frequency and a particular spatial frequency was inserted in a particular range bin. Reference data are selected from consecutive cells on each side of the cell-under-test (see Appendix for complete details on all schemes). We employ normalized test statistics, which provide a constant false alarm rate (CFAR) characteristic for homogenous clutter [7].

For each example, we provide plots of the magnitude of the normalized test statistics for a set of ranges including the target range. We judge a scheme by how large the test statistic is at the target range in comparison to other ranges.

In the first example, we inserted a target at range bin 150 for the cases shown in Table 1. The location of the targets and an estimate of the clutter (plus noise) power spectral density (psd) are illustrated in Fig. 1. As visible from Fig. 1, the psd estimate used is rather crude and is provided to give a rough description of the clutter environment. In the estimate no neighboring range cells are averaged and a Blackman window is used. Some of the artifacts can be removed by averaging, but this was not considered necessary in this case.

| Case | Normalized Doppler Frequency | Normalized Spatial Frequency |
|---|---|---|
| **a** | -0.2656 | -0.2656 |
| **b** | -0.0312 | -0.0312 |
| **c** | 0.125 | 0.203 |
| **d** | -0.0312 | -0.1875 |
| **e** | -0.0312 | 0.203 |
| **f** | 0.3593 | -0.1875 |
| **g** | -0.1875 | 0.3593 |

**Table 1** ) Test cases for each example.

A summary of the results is given in Table 2. Fig. 2 through Fig. 8 presents the results for most of the schemes tested. FTS and subarraying FTS generally perform poorly, so their results are not shown. In this example, generally JDL provides best results. JDL is best in every case except cases d and e. In case d, BeamAD slightly outperforms JDL and ADPCA, but the difference is quite small. In case e, EFA outperforms the other schemes, however JDL also performs well. The apparently large interference indicated by Fig. 1 near the normalized Doppler frequency -0.0312 could be the reason why JDL is not best in these two cases. These are apparently difficult cases where no scheme can really excel. Table 2 shows that case b is also quite difficult, but here JDL performs much better than the other schemes. The extra clutter ridges in Fig. 1 are discussed in [8] and [9].

In the second example, we inserted a target at range bin 350. We present results for the same cases in Table 1. The best three schemes for all the cases are given in Table 3. The normalized test statistics for the six best schemes tested for each case in Table 1 are given in Figures 10 through 16. The results indicate that none of the schemes always outperforms all the others. However, post-Doppler algorithms are generally better than pre-Doppler algorithms. Either JDL or EFA were best in all but case b. In case b, where the target is inserted in the largest clutter of all cases, BEFA is only slightly better than EFA and JDL.

Next, we inserted a target at range bin 415. We present results for the same cases as in previous examples. The location of the targets and an estimate of the clutter psd is given in Fig.

17. A summary of the results is provided in Table 4. The normalized test statistics are given in Fig. 18 through Fig. 24. Here for cases b, c, d, f, and g either JDL, or BEFA provide best performance. In the other cases, EFA is best and JDL also performs well. JDL performs well in every case except case b. Even in this case, its performance is not bad. EFA and its beamspace version are best in some cases and near-best in others. ADPCA and its beamspace version give good performance in number of cases, but these schemes were never best in this example.

Finally, we test the same cases as before when the target is inserted in range bin 500. The locations of the targets and an estimate of the clutter psd is given in Fig. 18. A summary of the results is given in Table 5. Fig. 26 through Fig. 32 provide the test statistics for the six best schemes in each case. Again the beamspace post-doppler algorithms, JDL and BEFA, outperform the element space algorithms except for case e where ADPCA is best.

# 4. CONCLUSIONS

In our tests, JDL and EFA generally perform very well. Subarrayed EFA also shows good performance in many situations. The common element these schemes share is post doppler processing. This type of processing, used in the correct way, appears to be superior in these real data cases. This appears to be the major result of this study. To a much lesser extent, schemes which estimate fewer parameters (lower degree of freedom (DOF) schemes) do appear to provide some benefits in non-homogeneous cases. The number of parameters estimated for each scheme is listed in Appendix 1. Some further discussion and analysis of non-homogeneous cases is given in Appendix 2. When there is a strong interference near the target, as in case d and e in Table 5 for example, ADPCA performs well and sometimes outperforms all the other schemes. The reason appears to be related to the extra whitening provided by its steering vector.

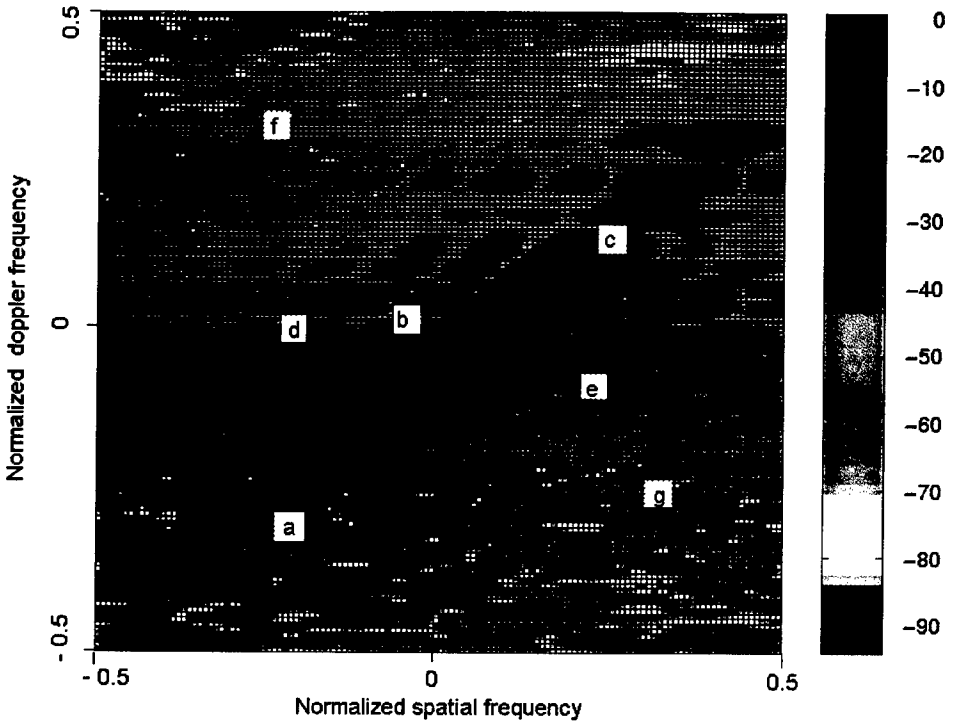


**Figure 1)** Power spectrum plot of range 150

| Case | Normalized Doppler Frequency | Normalized Spatial Frequency | The 3 best schemes | D | Figure |
|---|---|---|---|---|---|
| a | -0.2656 | -0.2656 | JDL<br>BEFA<br>BeamAD | 36<br>25<br>16 | 2 |
| b | -0.0312 | -0.0312 | JDL | 10 | 3 |
| c | 0.125 | 0.203 | JDL<br>EFA | 30<br>12 | 4 |
| d | -0.0312 | -0.1875 | BeamAD<br>JDL<br>ADPCA | 8<br>7<br>6 | 5 |
| e | -0.0312 | 0.203 | EFA<br>JDL<br>BeamAD | 20<br>12<br>5 | 6 |
| f | 0.3593 | -0.1875 | JDL<br>EFA<br>BeamAD | 43<br>38<br>30 | 7 |
| g | -0.1875 | 0.3593 | JDL<br>BEFA<br>BeamAD | 38<br>18<br>7 | 8 |

**Table 2)** The three best schemes for all the cases when the target is inserted at range 150. (D is the approximate difference between the normalized test statistic at the target and the largest peak in the normalized test statistic at some other range)

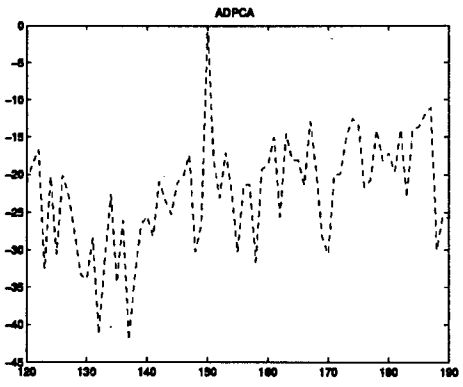


a) ADPCA

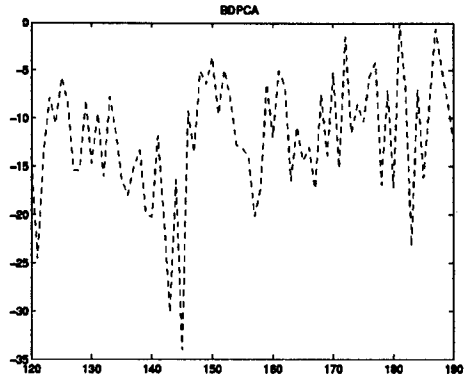


b) BDPCA

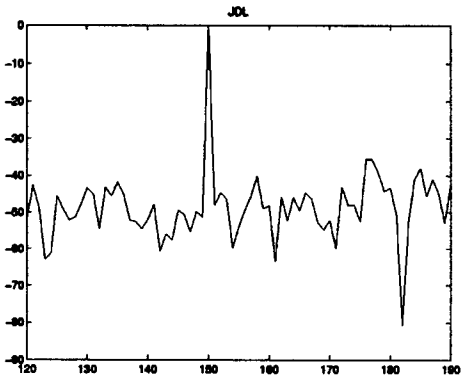


c) JDL

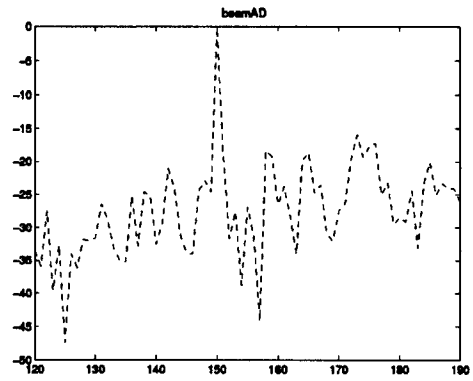


d) BeamAD

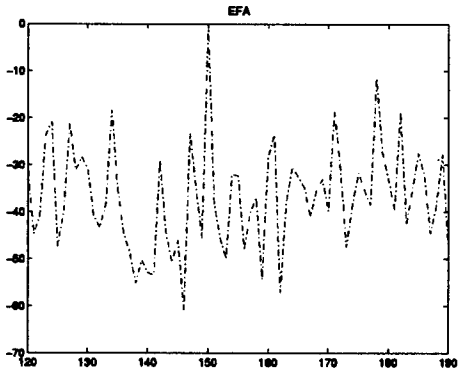


e) EFA

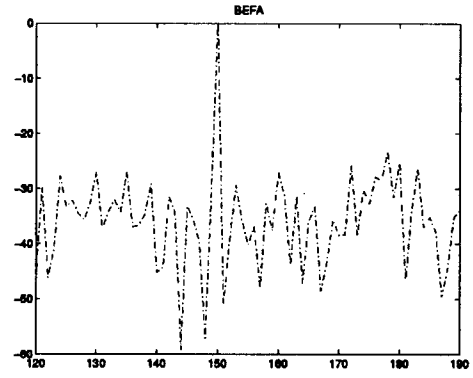


f) BEFA

**Figure 2)** Performance comparison when target is inserted at range150, case a.

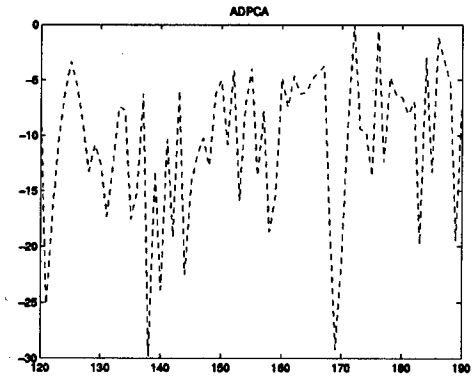


a) ADPCA

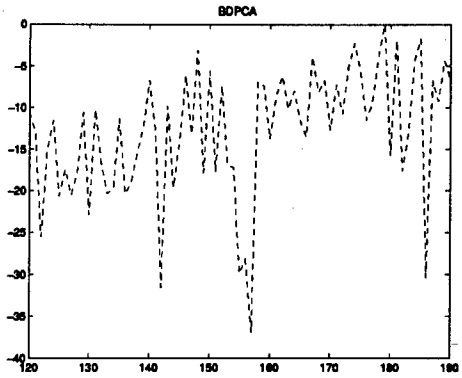


b) BDPCA

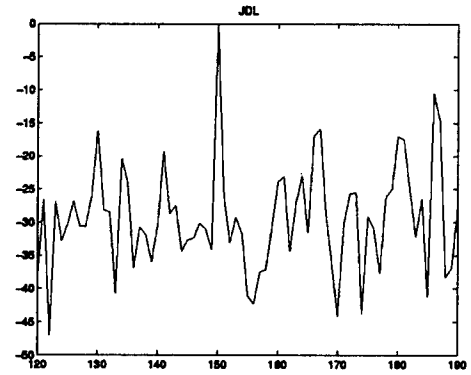


c) JDL

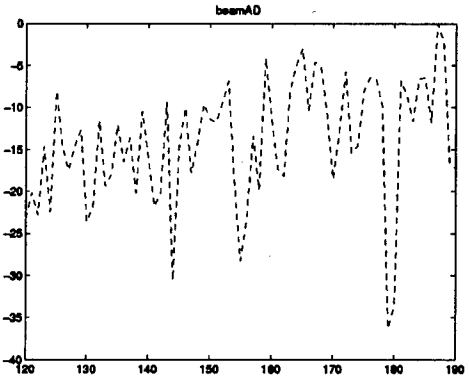


d) BeamAD

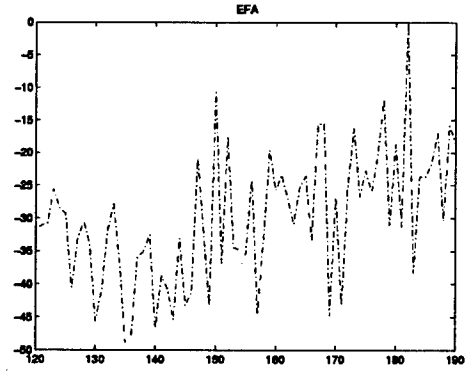


e) EFA

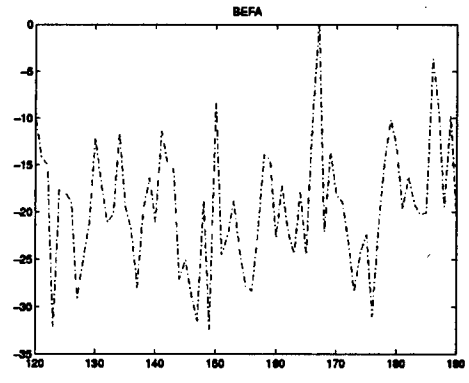


f) BEFA

**Figure 3)** Performance comparison when target is inserted at range 150, case b.

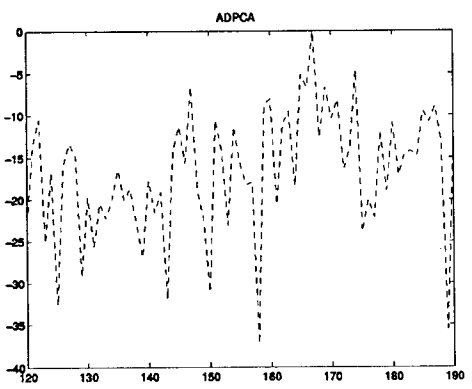


a) ADPCA

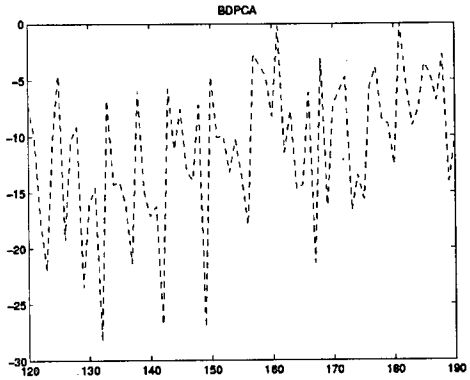


b) BDPCA

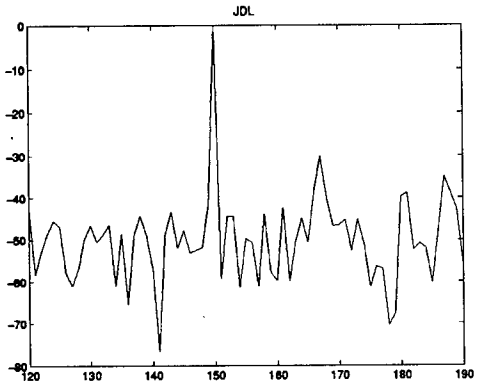


c) JDL

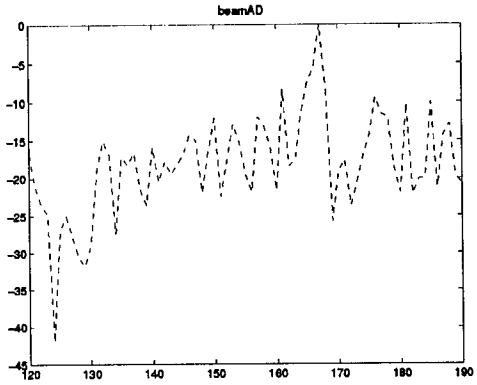


d) BeamAD

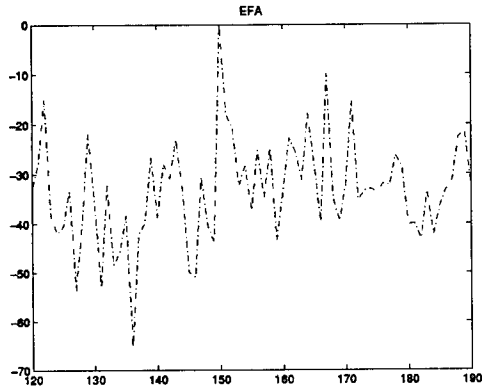


e) EFA

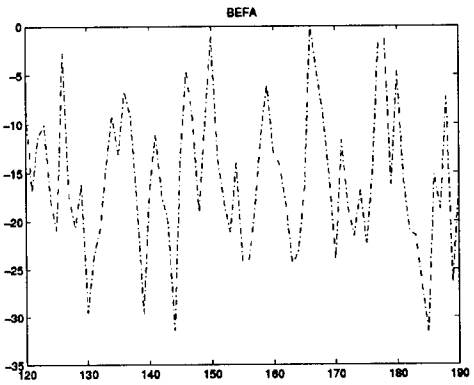


f)BEFA

**Figure4)** Performance comparison when target is inserted at range 150, case c.

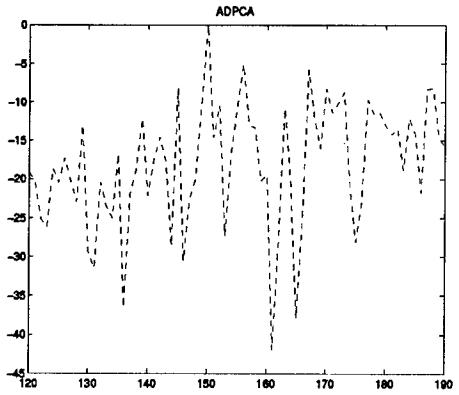


a) ADPCA

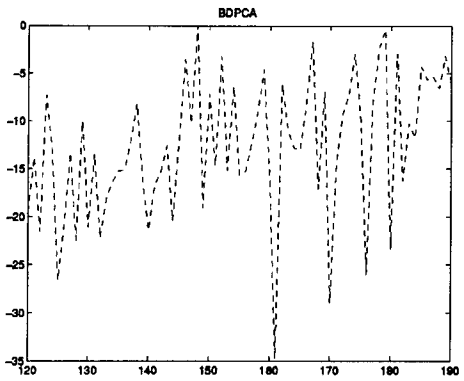


b) BDPCA

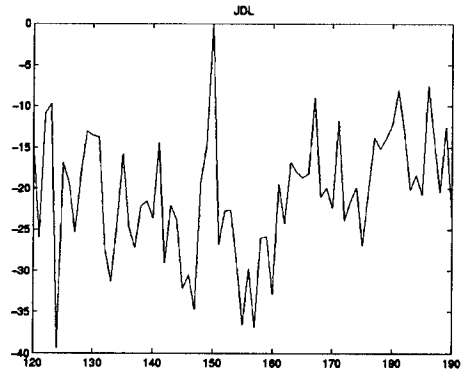


c) JDL

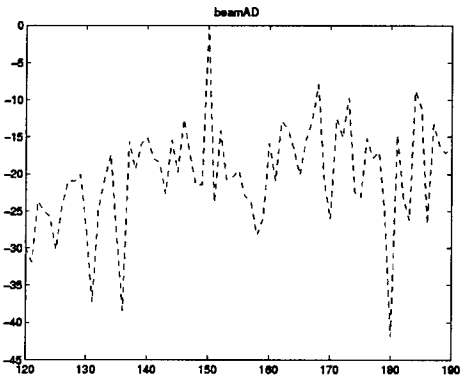


d) BeamAD

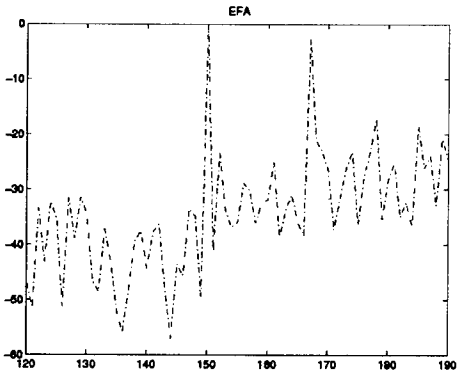


e) EFA

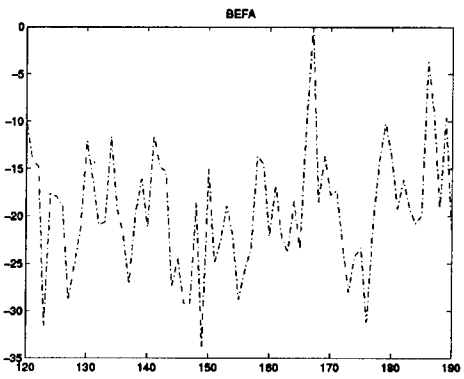


f) BEFA

**Figure 5)** Performance comparison when target is inserted at range 150, case d.

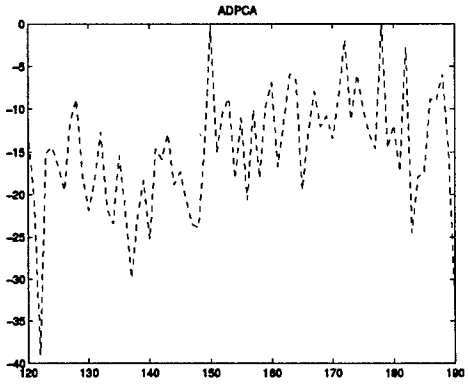


a) ADPCA

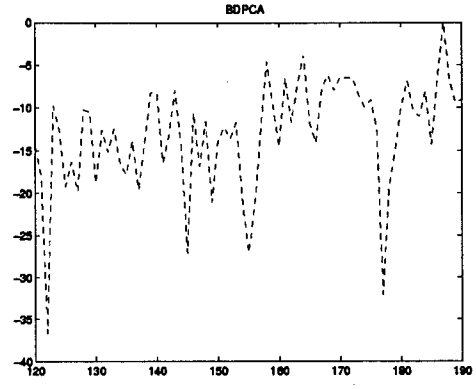


b) BDPCA

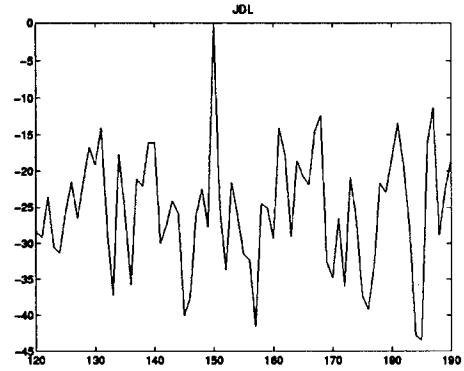


c) JDL

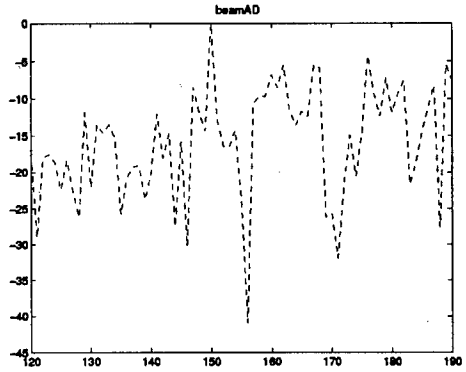


d) BeamAD

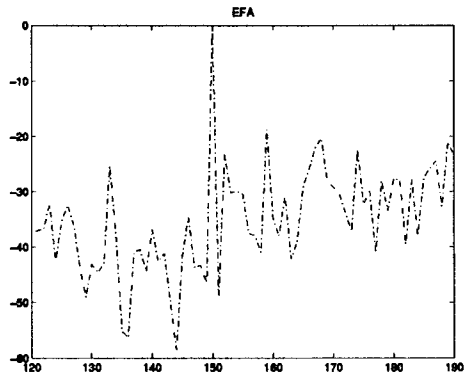


e) EFA

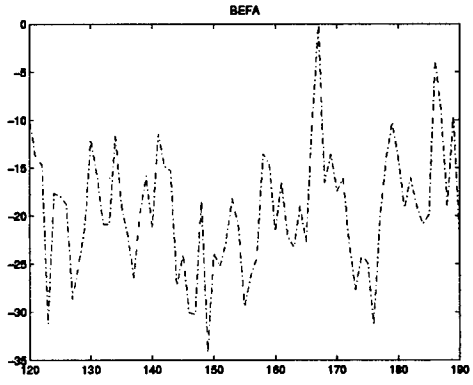


f) BEFA

**Figure 6)** Performance comparison when target is inserted at range 150, case e.

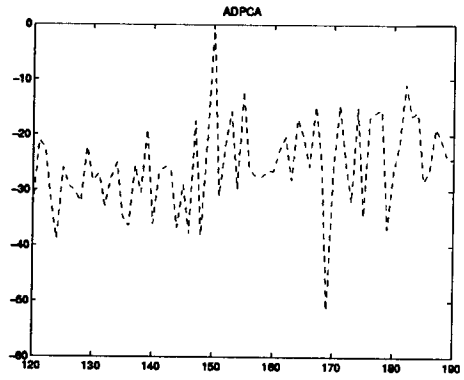


a) ADPCA

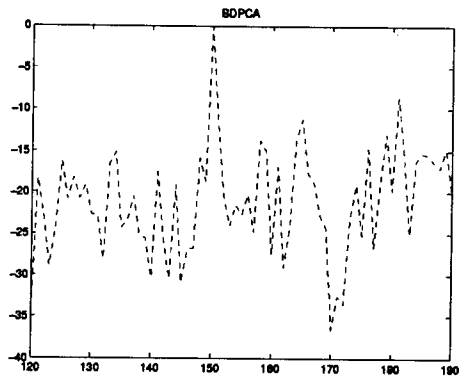


b) BDPCA

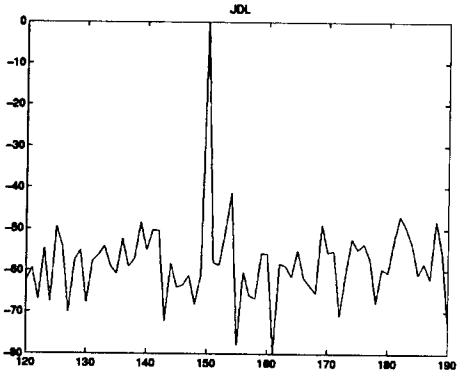


c) JDL

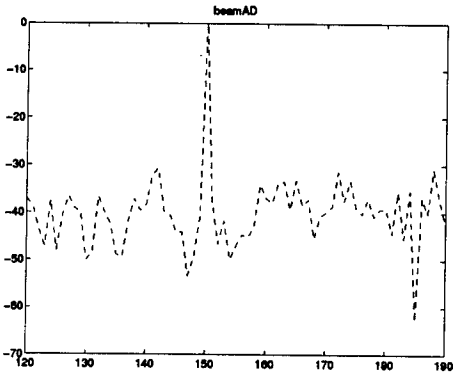


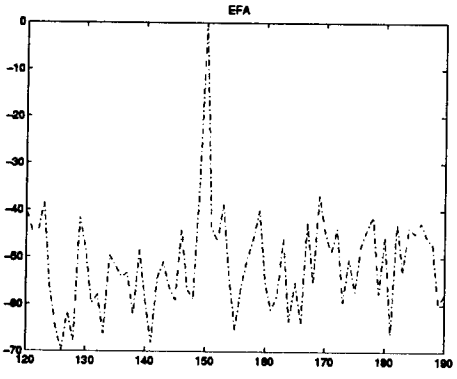


e) EFA

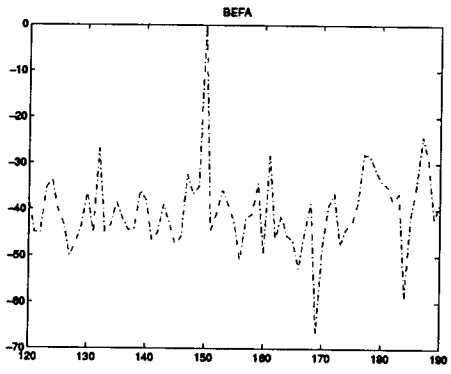


f) BEFA

**Figure 7)** Performance comparison when target is inserted at range 150, case f.

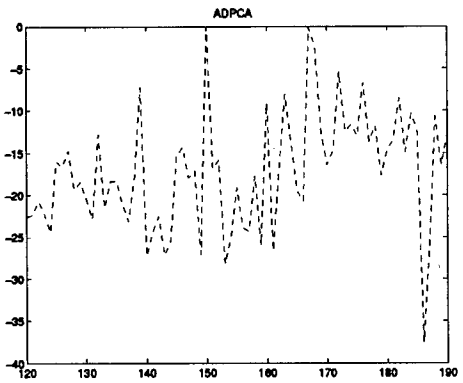


a) ADPCA

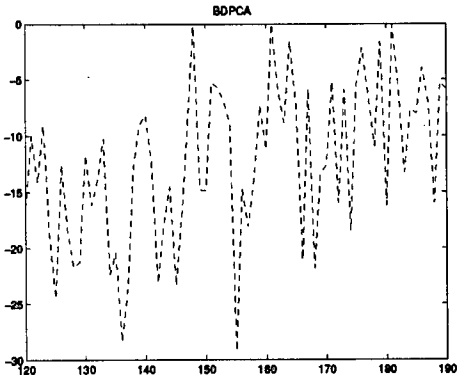


b) BDPCA

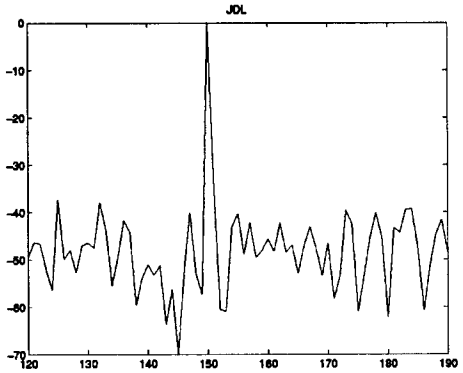


c) JDL

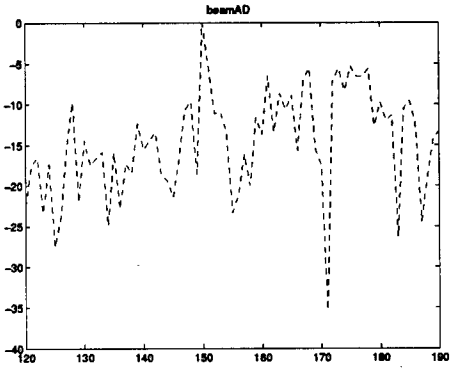


d) BeamAD

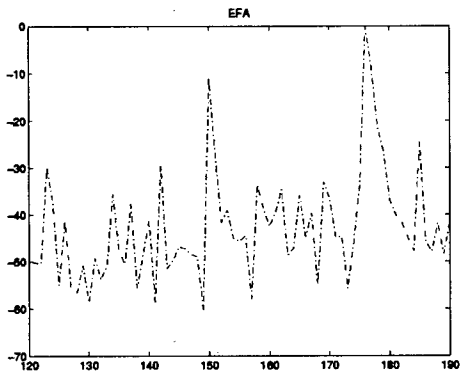


e) EFA

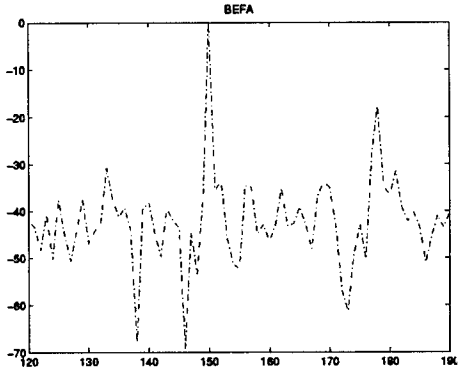


f) BEFA

**Figure 8)** Performance comparison when target is inserted at range 150, case g.

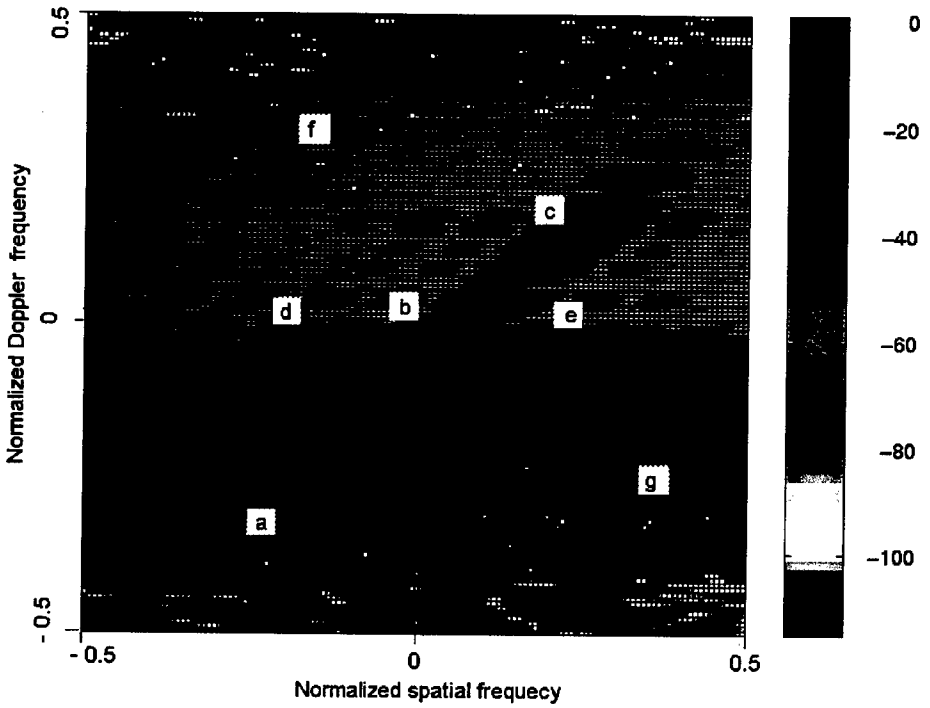


**Figure 9)** Power spectrum plot of range 350.

| Case | Normalized Doppler Frequency | Normalized Spatial Frequency | The 3 best schemes | D | Figure |
|---|---|---|---|---|---|
| a | -0.2656 | -0.2656 | EFA<br>JDL<br>BEFA | 24<br>18<br>5 | 10 |
| b | -0.0312 | -0.0312 | BEFA<br>EFA<br>JDL | 15<br>12<br>10 | 11 |
| c | 0.125 | 0.203 | JDL<br>EFA<br>BEFA | 34<br>25<br>13 | 12 |
| d | -0.0312 | -0.1875 | EFA<br>JDL<br>ADPCA | 28<br>20<br>12 | 13 |
| e | -0.0312 | 0.203 | EFA<br>JDL<br>ADPCA | 22<br>18<br>7 | 14 |
| f | 0.3593 | -0.1875 | EFA<br>JDL<br>BeamAD | 48<br>43<br>24 | 15 |
| g | -0.1875 | 0.3593 | JDL<br>BEFA<br>BeamAD | 33<br>18<br>14 | 16 |

**Table 3)** The three best schemes for all the cases when the target is inserted at range 350. (D is the approximate difference between the normalized test statistic at the target and the largest peak in the normalized test statistic at some other range.)

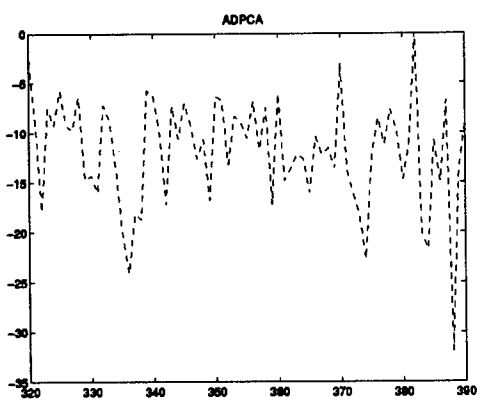


a) ADPCA

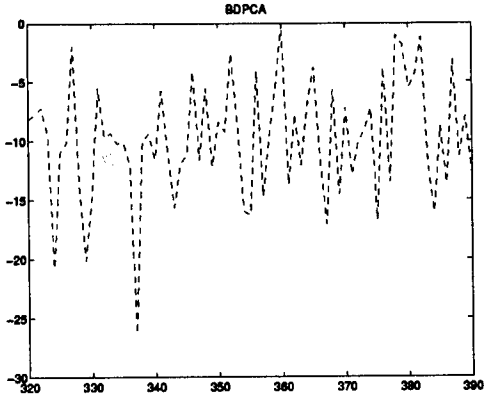


b) BDPCA

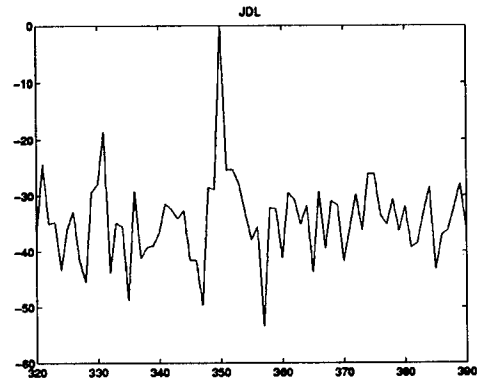


c) JDL

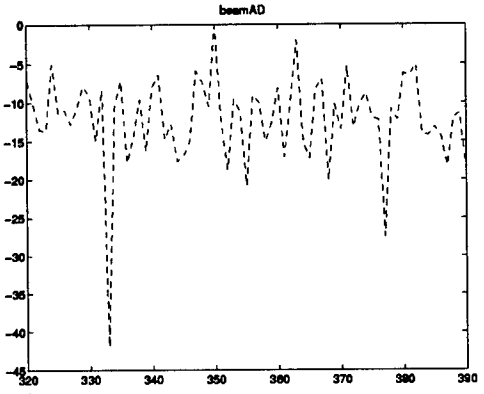


d) BeamAD

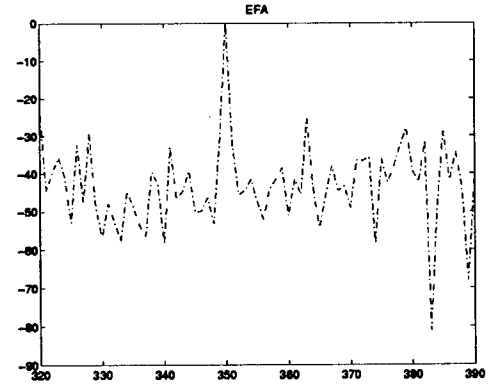


e) EFA

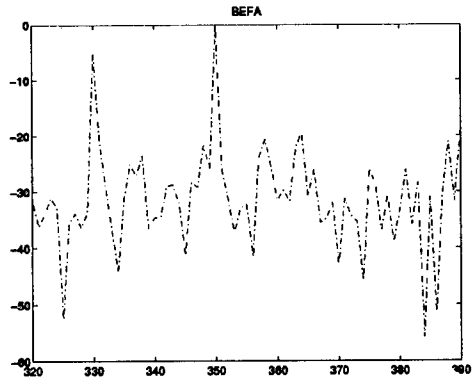


f) BEFA

**Figure 10)** Performance comparison when target is inserted at range 350, case a.

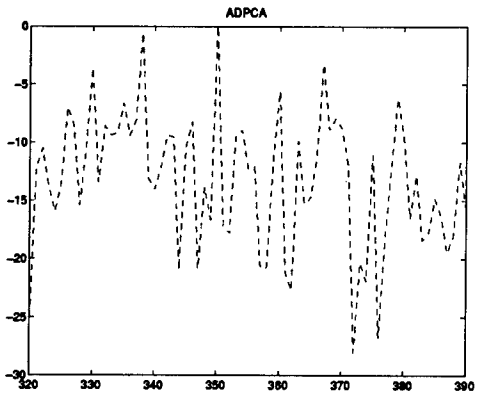


a) ADPCA

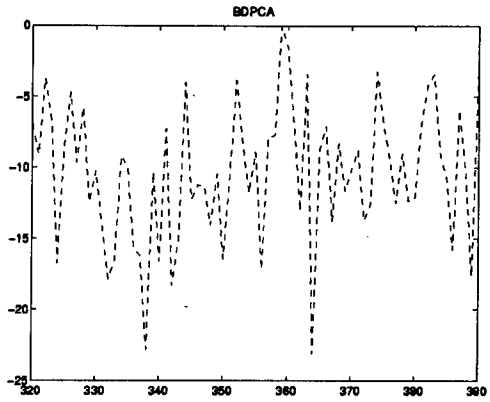


b) BDPCA

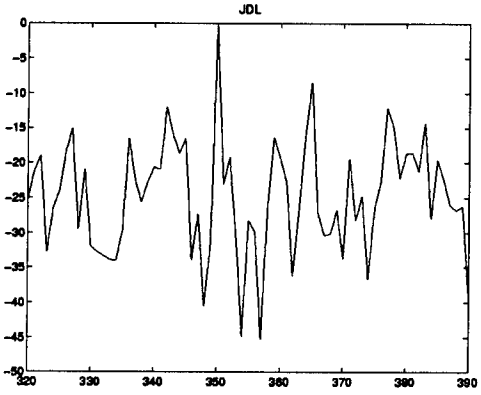


c) JDL

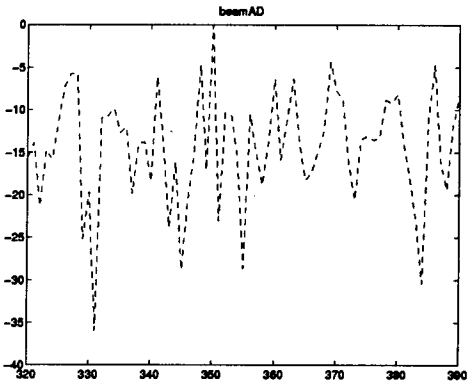


d) BeamAD

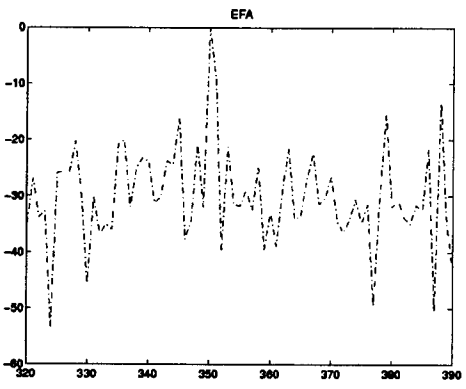


e) EFA

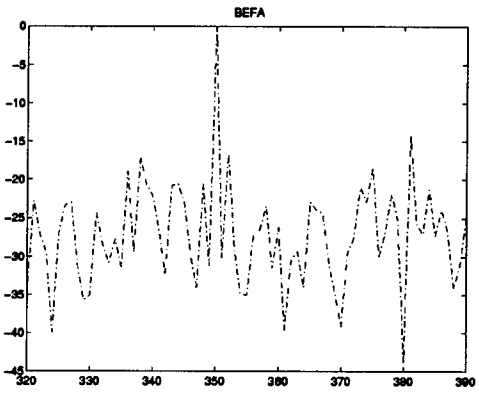


f) BEFA

**Figure11)** Performance comparison when target is inserted at range 350, case b.

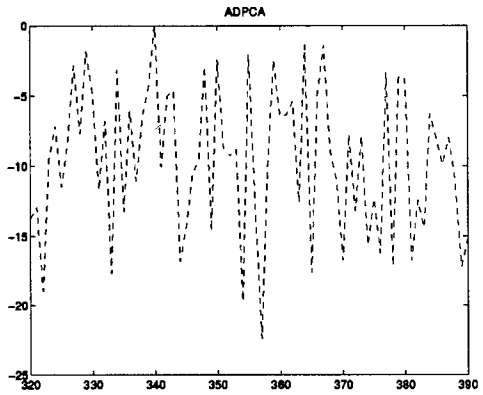


a) ADPCA

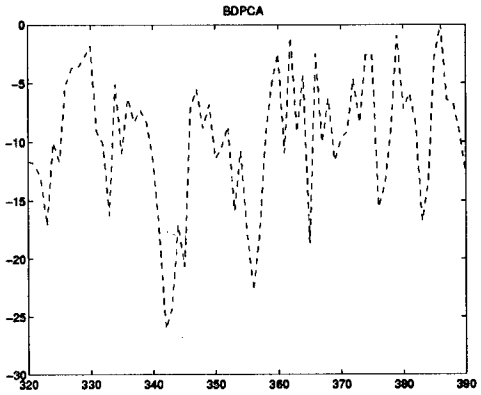


b) BDPCA

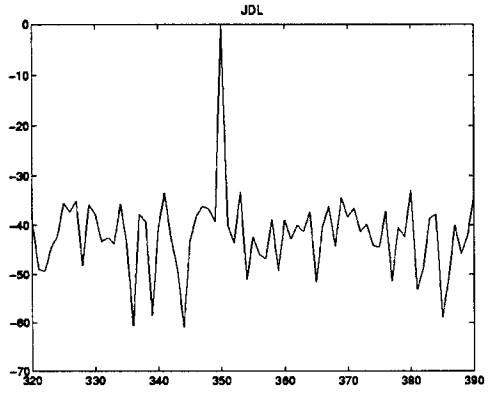


c) JDL

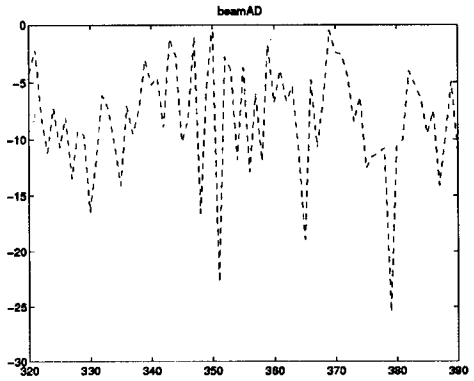


d) BeamAD

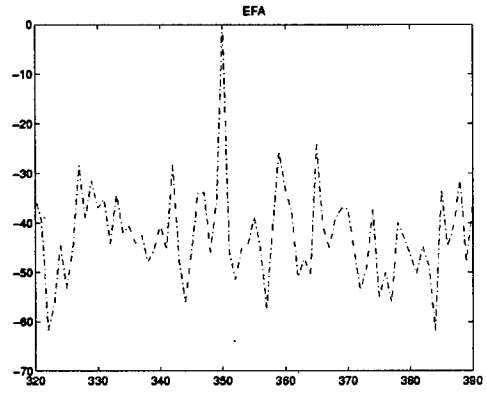


e) EFA

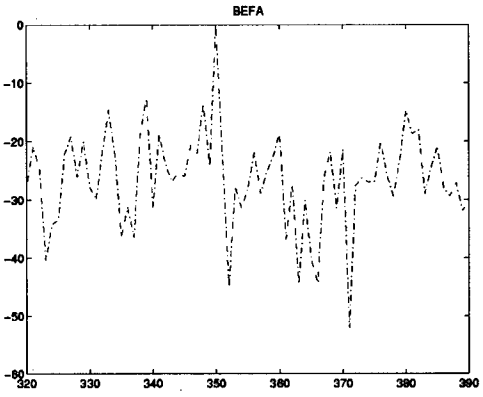


f) BEFA

**Figure 12)** Performance comparison when target is inserted at range 350, case c.

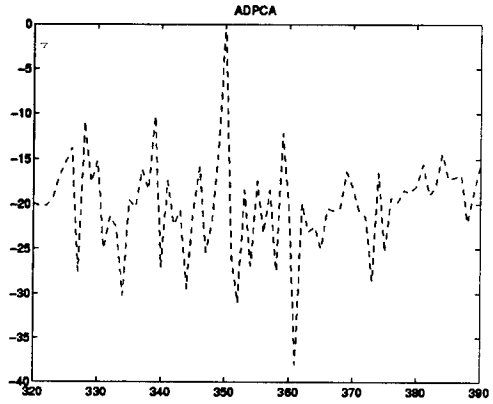


a) ADPCA

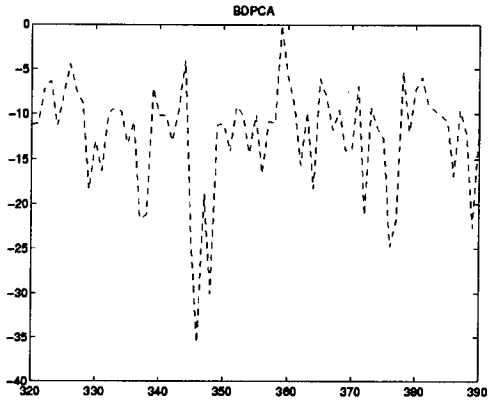


b) BDPCA

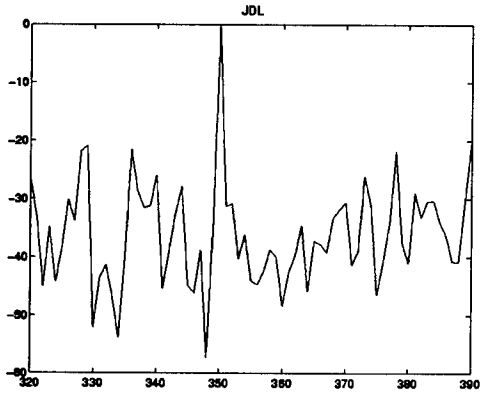


c) JDL

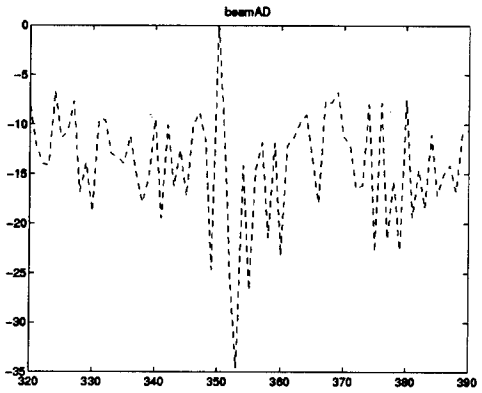


d) BeamAD

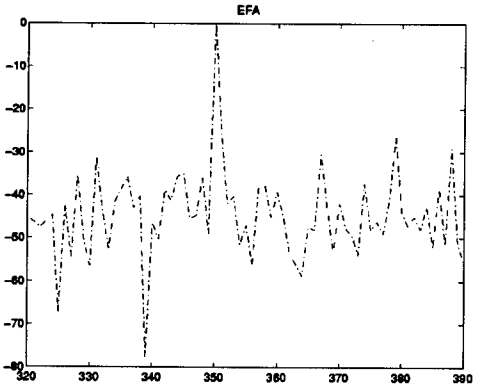


e) EFA

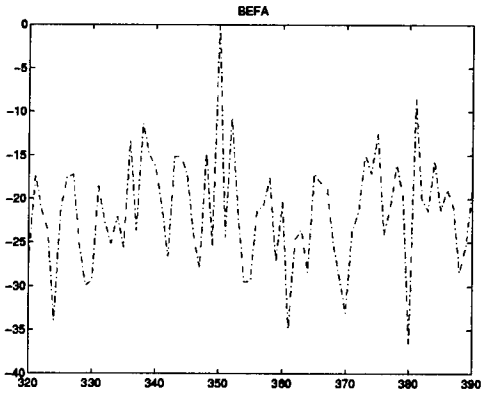


f) BEFA

**Figure 13)** Performance comparison when target is inserted at range 350, case d.

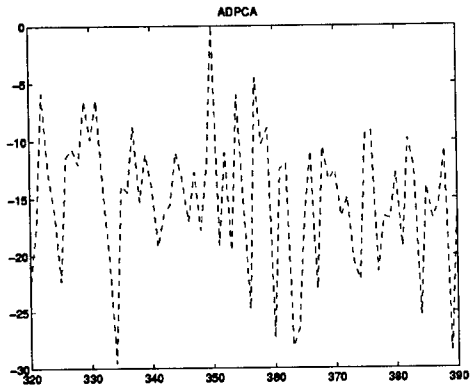


a) ADPCA

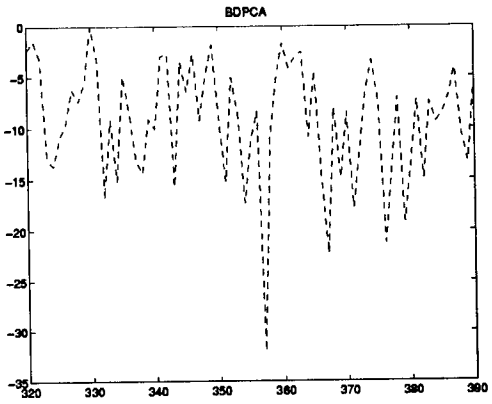


b) BDPCA

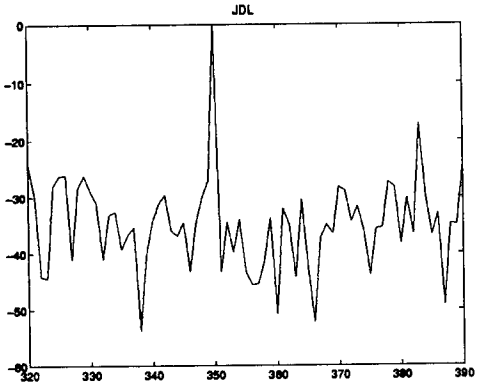


c) JDL

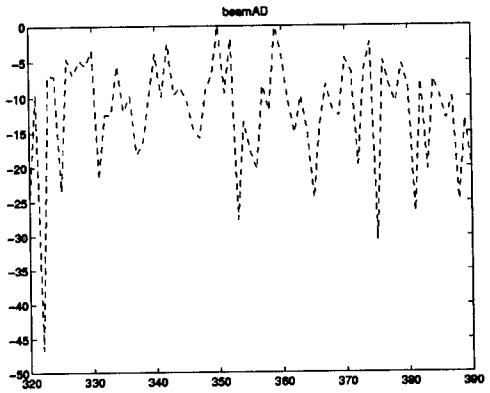


d) BeamAD

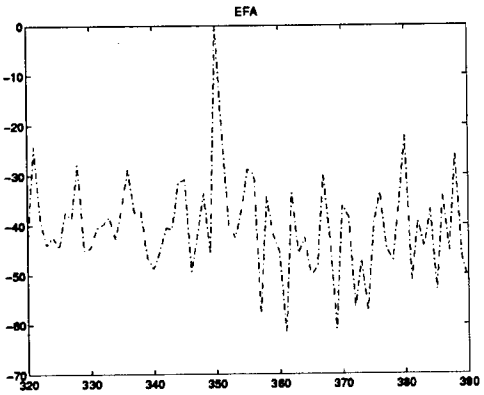


e) EFA

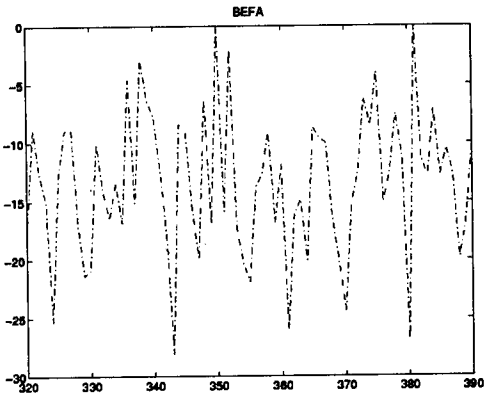


f) BEFA

**Figure 14)** Performance comparison when target is inserted at range 350, case e.

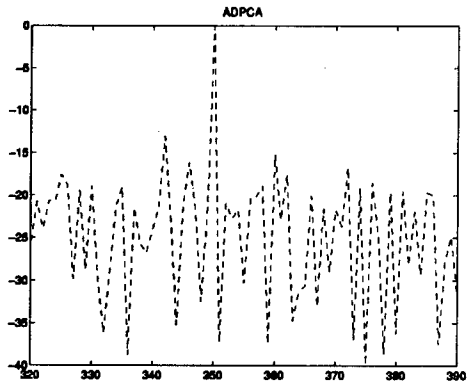


a) ADPCA

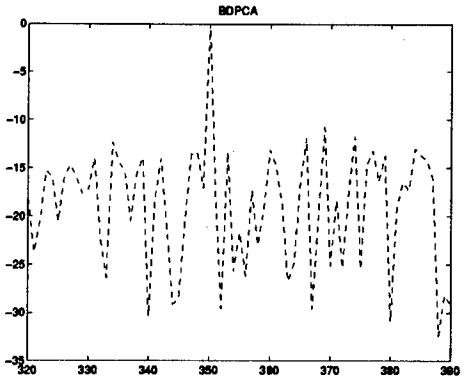


b) BDPCA

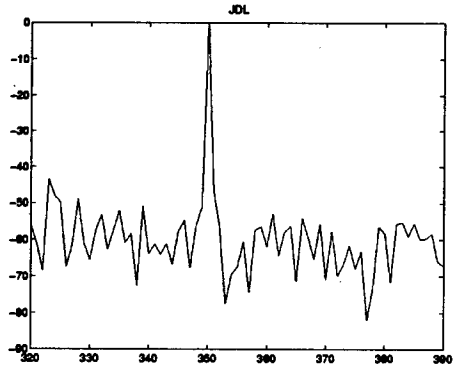


c) JDL

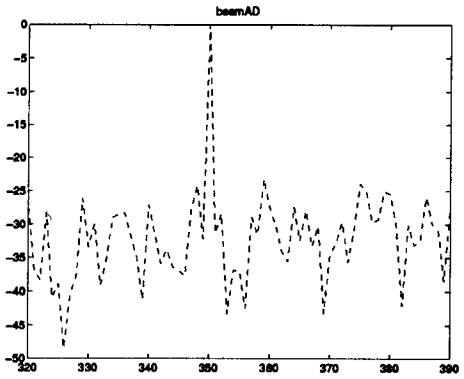


d) BeamAD

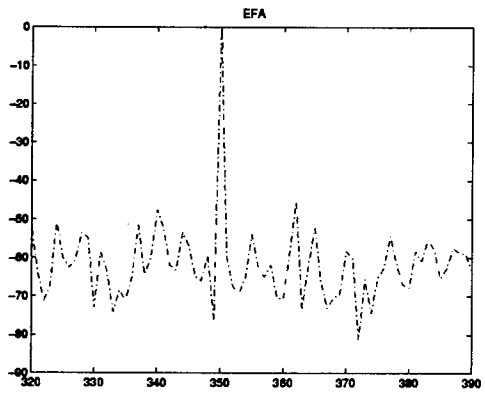


e) EFA

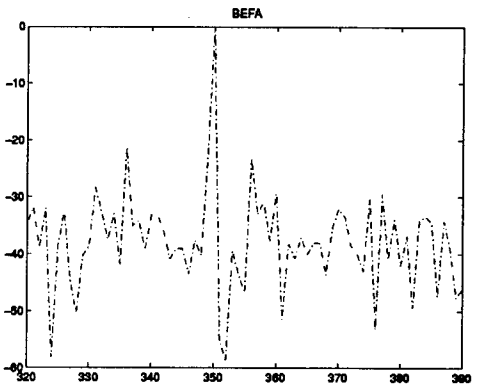


f) BEFA

**Figure 15)** Performance comparison when target is inserted at range 350, case f.

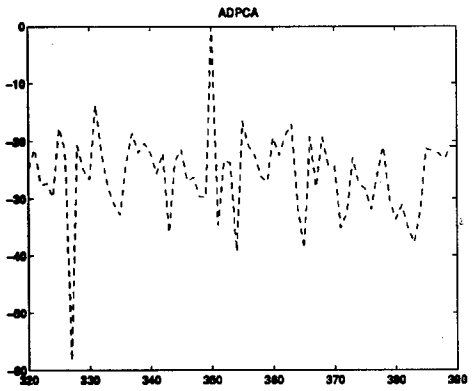


a) ADPCA

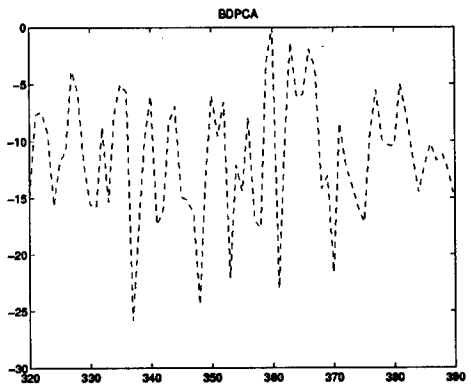


b) BDPCA

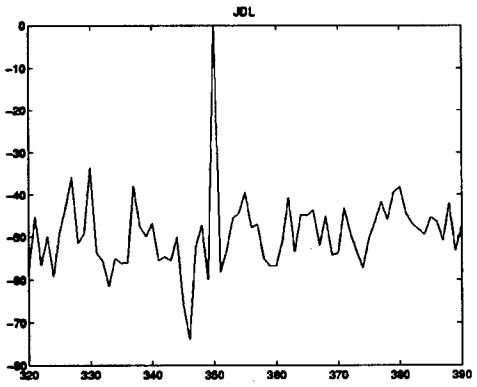


c) JDL

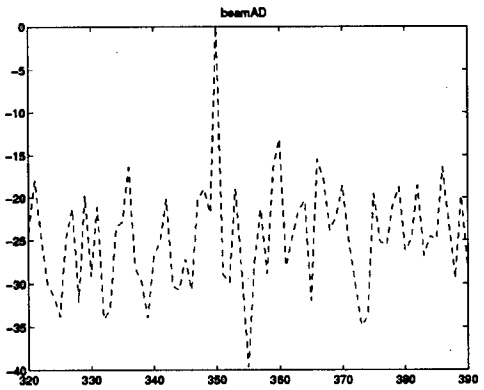


d) BeamAD

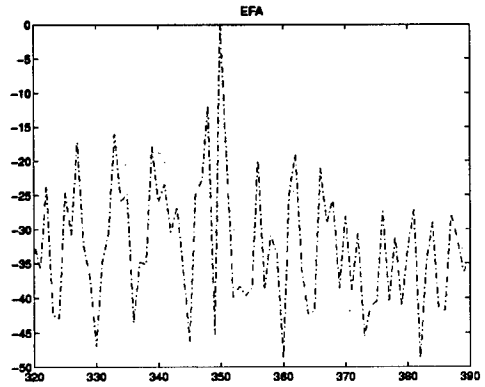


e) EFA

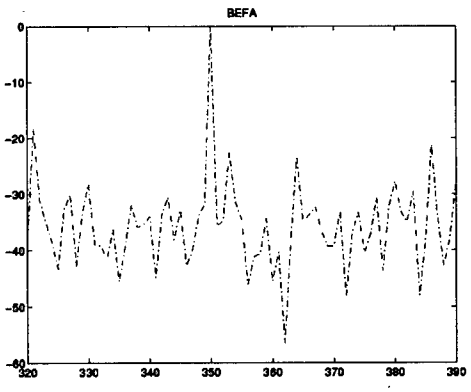


f) BEFA

**Figure16)** Performance comparison when target is inserted at range 350, case g.

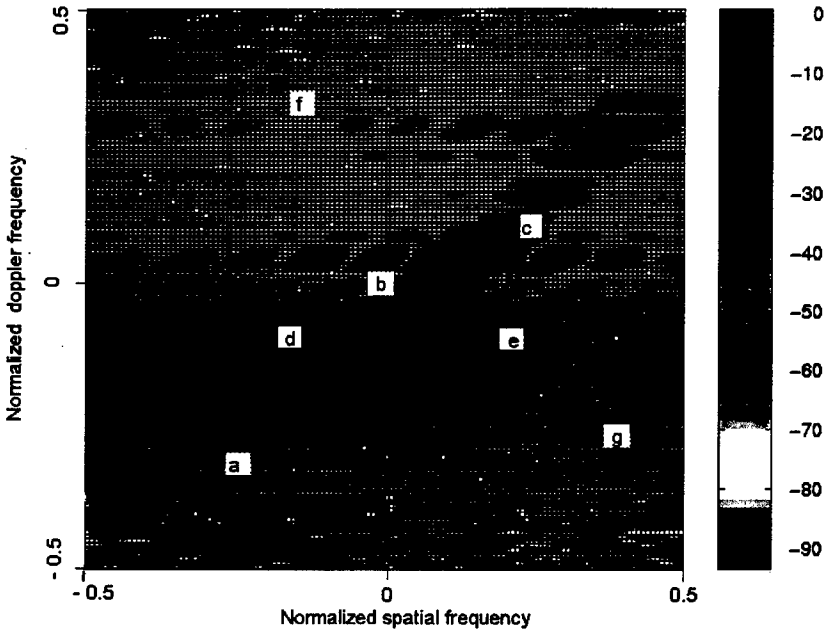


**Figure 17)** Power spectrum plot of range 415

| Case | Normalized Doppler Frequency | Normalized Spatial Frequency | The 3 best schemes | D | Figure |
|---|---|---|---|---|---|
| a | -0.2656 | -0.2656 | EFA<br>JDL<br>ADPCA | 25<br>22<br>12 | 18 |
| b | -0.0312 | -0.0312 | BEFA<br>BeamAD<br>EFA, ADPCA | 25<br>18<br>15 | 19 |
| c | 0.125 | 0.203 | BEFA<br>JDL<br>BeamAD | 30<br>23<br>12 | 20 |
| d | -0.0312 | -0.1875 | JDL, BEFA<br>BeamAD<br>EFA, ADPCA | 20<br>18<br>16 | 21 |
| e | -0.0312 | 0.203 | EFA<br>JDL<br>ADPCA | 28<br>24<br>15 | 22 |
| f | 0.3593 | -0.1875 | JDL<br>BeamAD<br>BEFA | 45<br>35<br>32 | 23 |
| g | -0.1875 | 0.3593 | JDL<br>EFA<br>BeamAD | 42<br>20<br>18 | 24 |

**Table 4)** The three best schemes for all the cases when the target is inserted at range 415. (D is the approximate difference between the normalized test statistic at the target and the largest peak in the normalized test statistic at some other range)

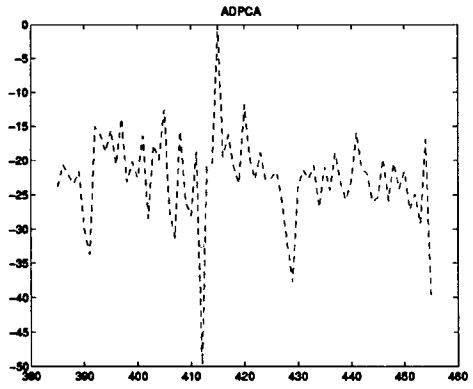


a) ADPCA

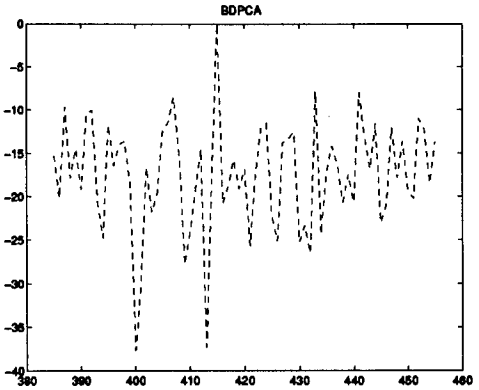


b) BDPCA

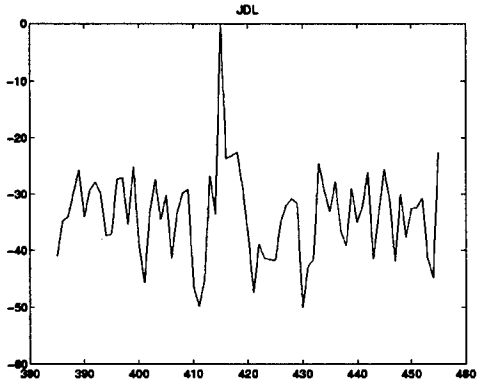


c) JDL

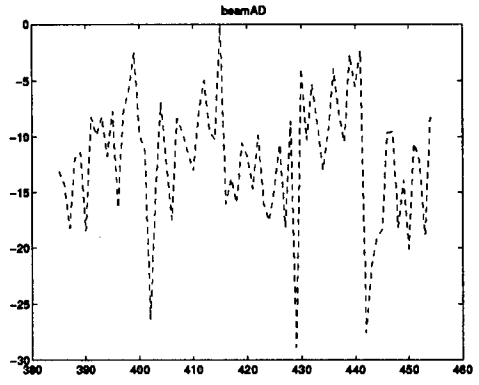


d) BeamAD

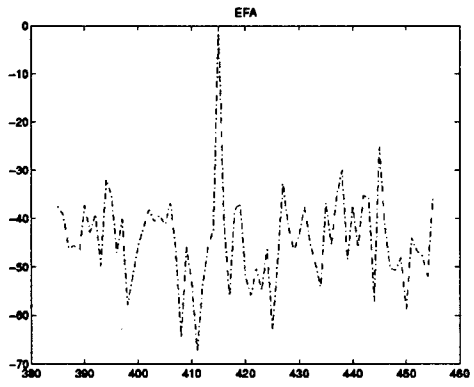


e) EFA

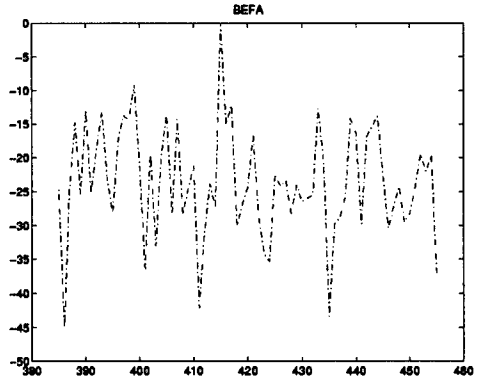


f) BEFA

**Figure18)** Performance comparison when target is inserted at range 415, case a.

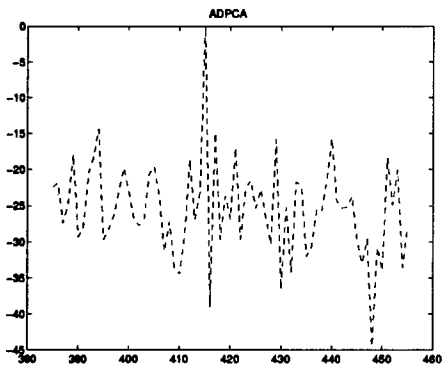


a) ADPCA

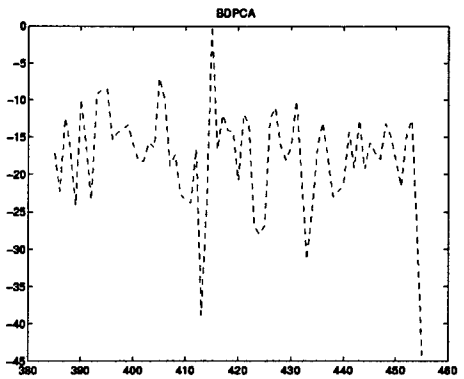


b) BDPCA

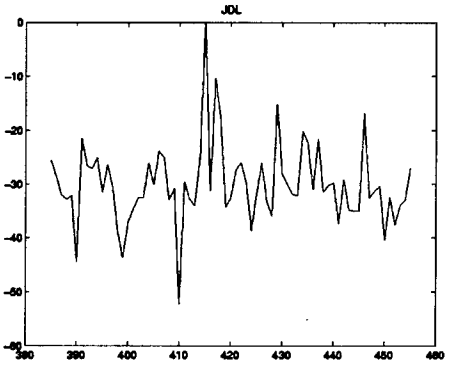


c) JDL

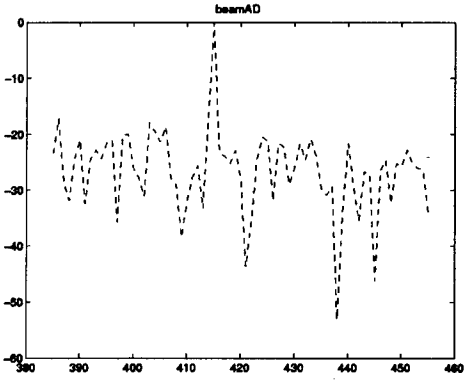


d) BeamAD

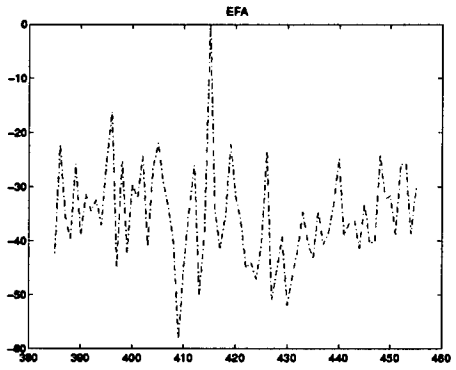


e) EFA

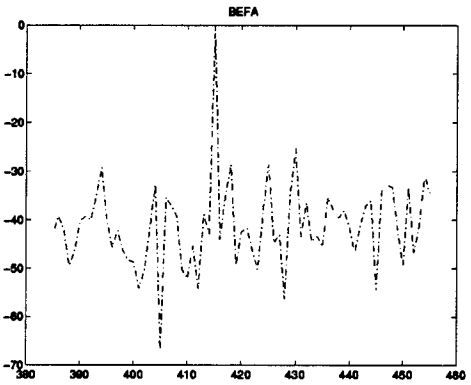


f)BEFA

**Figure 19)** Performance comparison when target is inserted at range 415, case b.

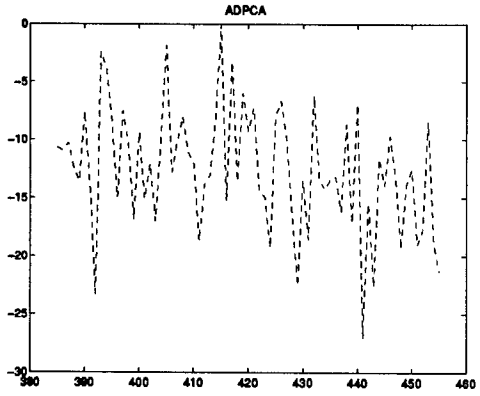


a) ADPCA

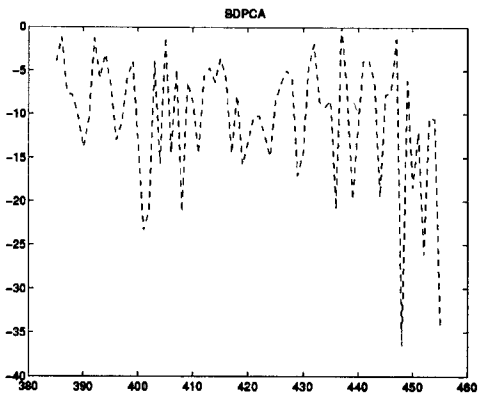


b) BDPCA

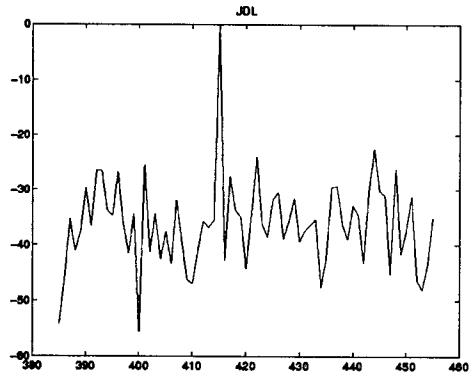


c) JDL

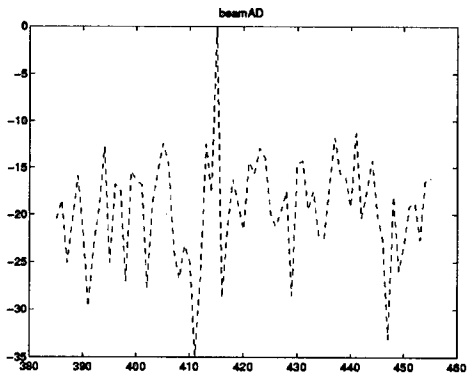


d) BeamAD

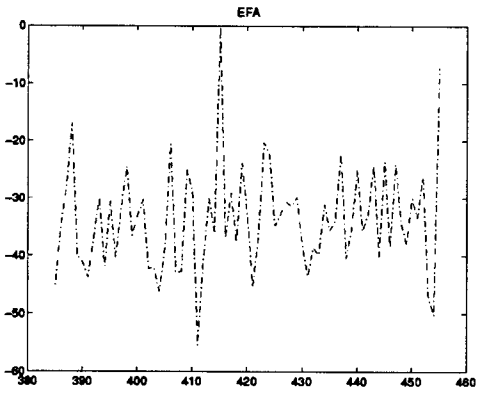


e) EFA

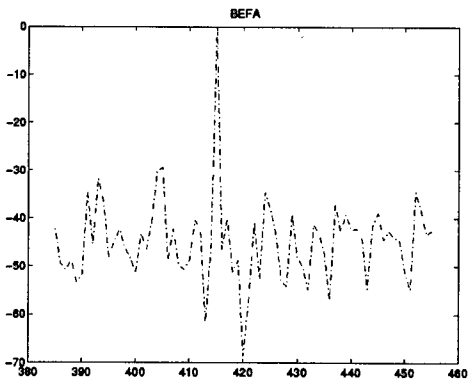


f) BEFA

**Figure 20)** Performance comparison when target is at range 415, case c.

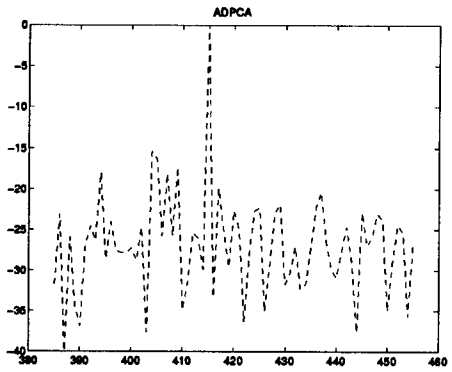


a) ADPCA

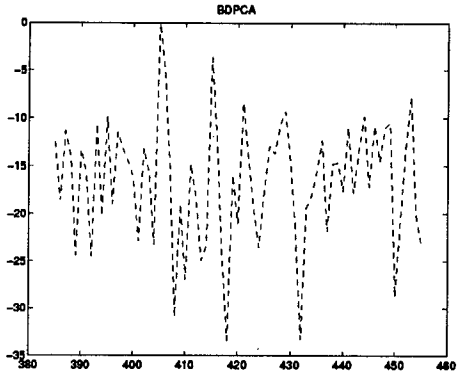


b) BDPCA

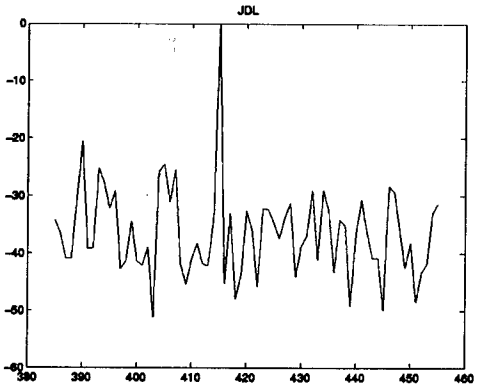


c) JDL

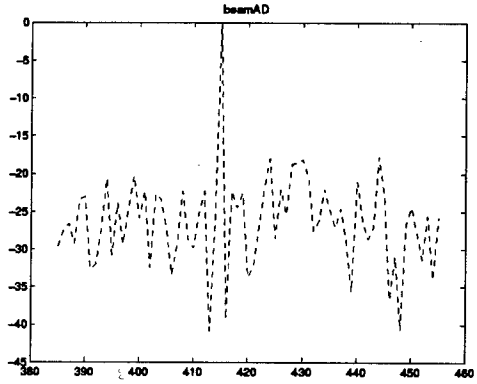


d) BeamAD

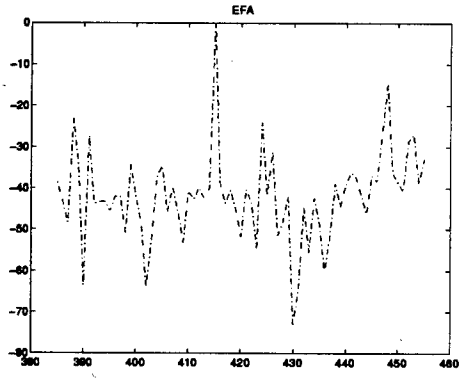


e) EFA

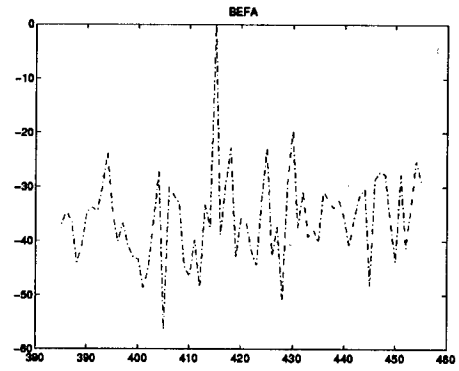


f) BEFA

**Figure 21)** Performance comparison when target is inserted at target range 415, case d.

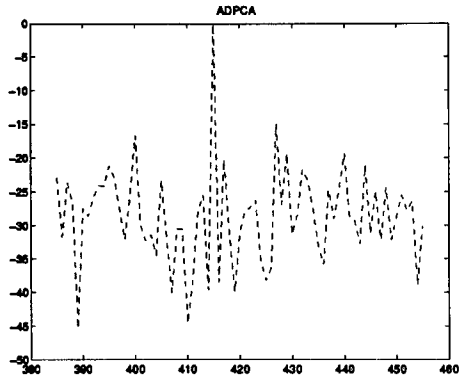


a) ADPCA

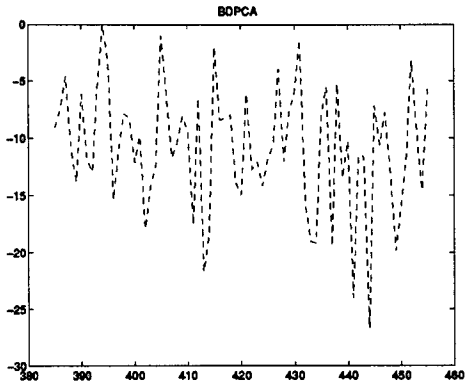


b) BDPCA

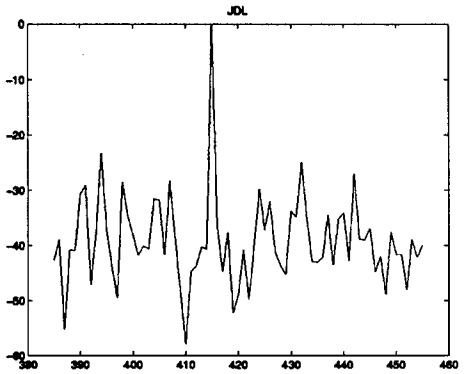


c) JDL

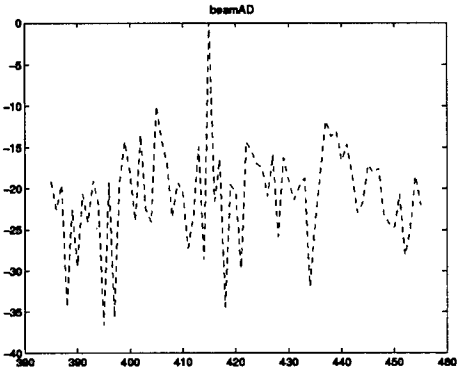


d) BeamAD

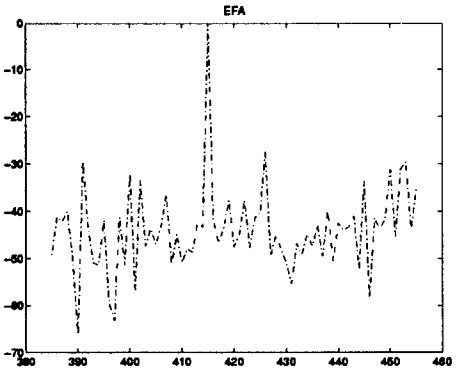


e) EFA

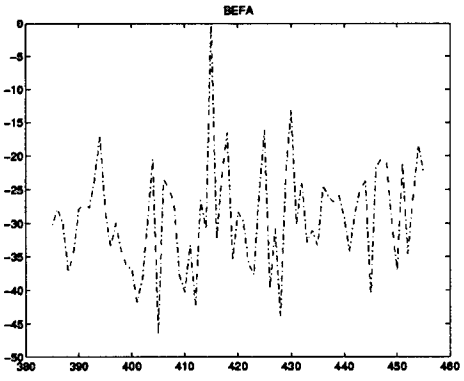


f) BEFA

**Figure 22)** Performance comparison when target is inserted at range 415, case e.

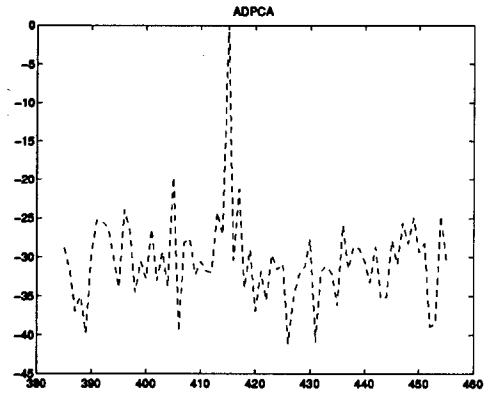


a) ADPCA

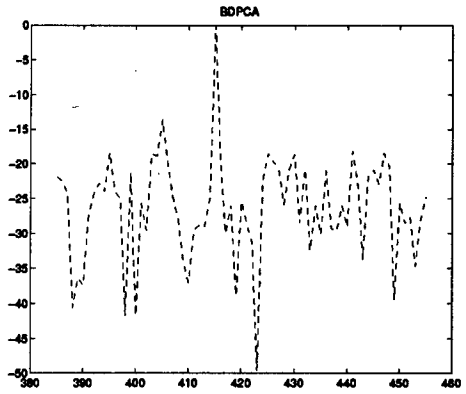


b) BDPCA

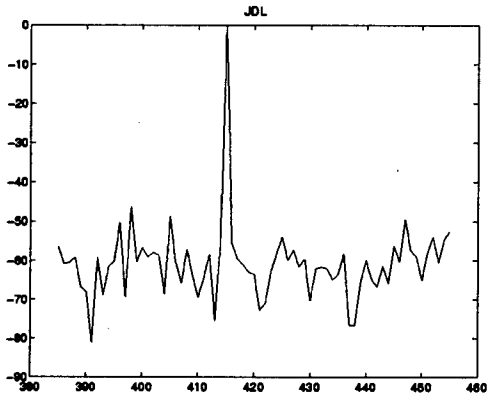


c) JDL

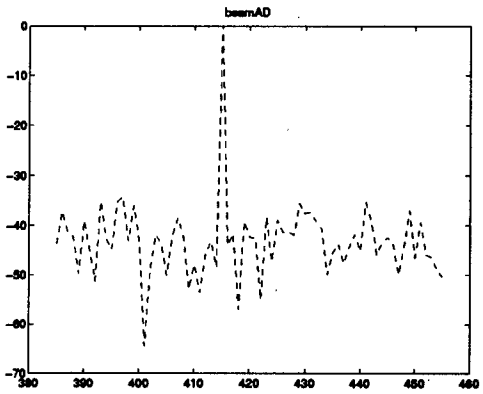


d) BeamAD

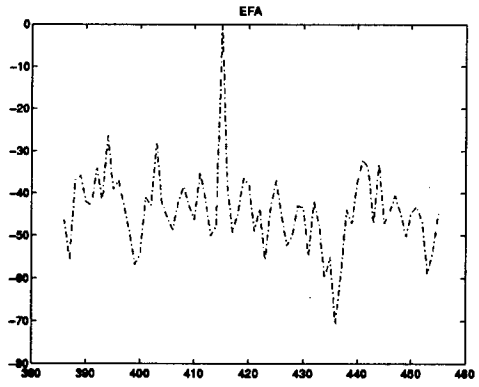


e) EFA

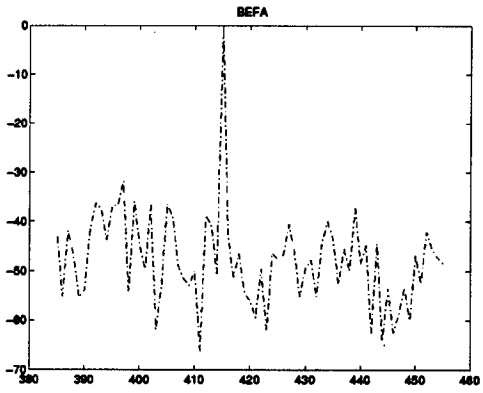


f) BEFA

**Figure 23)** Performance comparison when target is inserted at range 415, case f.

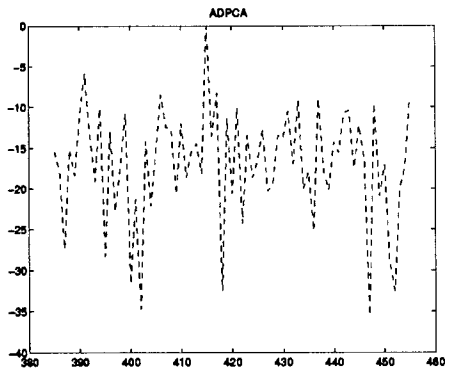


a) ADPCA

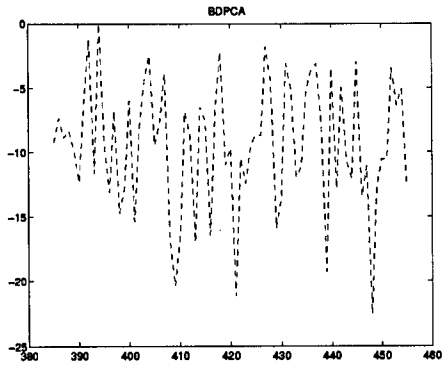


b) BDPCA

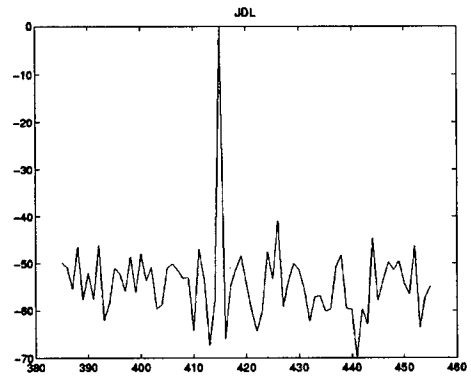


c)JDL

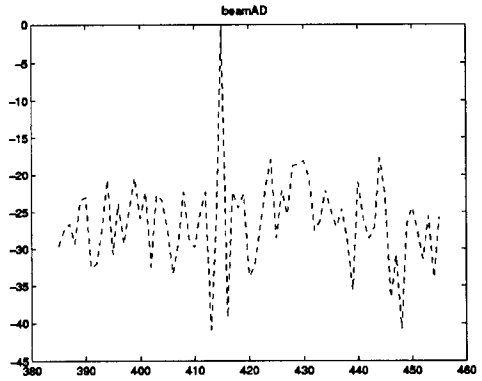


d)BeamAD

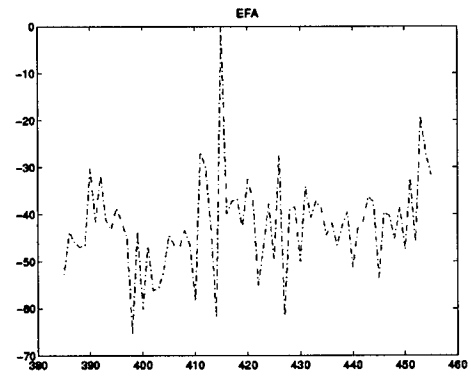


e)EFA

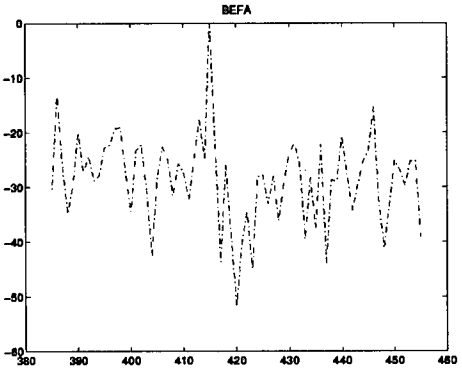


f)BEFA

**Figure 24)** Performance comparison when target is inserted at range 415, case g.

THIS PAGE INTENTIONALLY LEFT BLANK

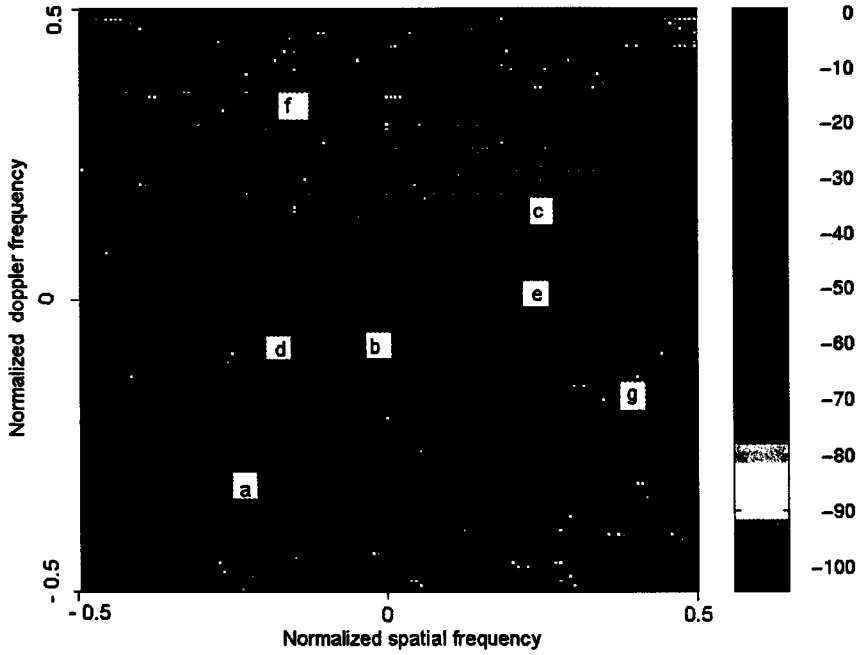


**Figure 25)** Power spectrum plot of range 500

| Case | Normalized Doppler Frequency | Normalized Spatial Frequency | The 3 best schemes | D | Figure |
|---|---|---|---|---|---|
| a | - 0.2656 | - 0.2656 | JDL<br>EFA<br>ADPCA | 32<br>13<br>7 | 26 |
| b | - 0.0312 | - 0.0312 | JDL<br>EFA<br>BEFA | 22<br>20<br>15 | 27 |
| c | 0.125 | 0.203 | JDL<br>BEFA<br>EFA,<br>BeamAD | 36<br>12<br>7 | 28 |
| d | - 0.0312 | - 0.1875 | JDL<br>EFA<br>ADPCA | 26<br>20<br>10 | 29 |
| e | - 0.0312 | 0.203 | ADPCA<br>JDL<br>EFA | 22<br>18<br>15 | 30 |
| f | 0.3593 | - 0.1875 | JDL<br>EFA, BEFA<br>BeamAD | 38<br>28<br>23 | 31 |
| g | - 0.1875 | 0.3593 | BEFA, JDL<br>BeamAD<br>EFA | 33<br>17<br>15 | 32 |

**Table 5)** The three best schemes for all the cases when the target is inserted at range 500. (D is the approximate difference between the normalized test statistic at the target peak and the largest peak in the normalized test statistic at some other range)

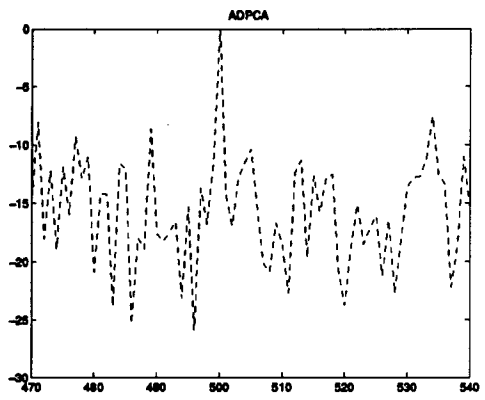


a) ADPCA

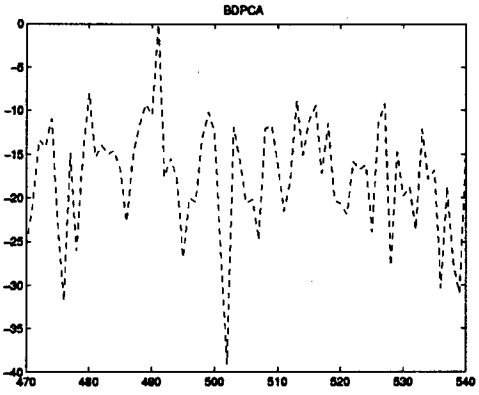


b) BDPCA

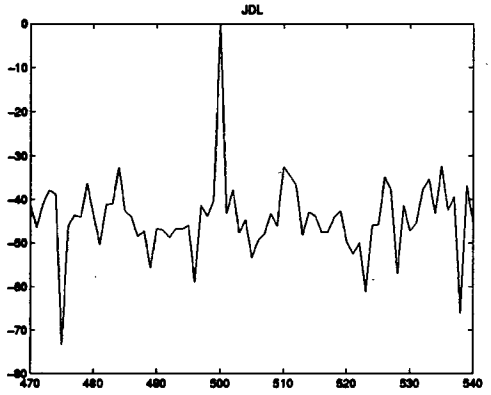


c) JDL

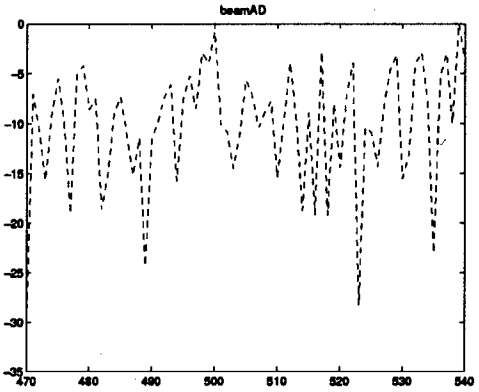


d) BeamAD

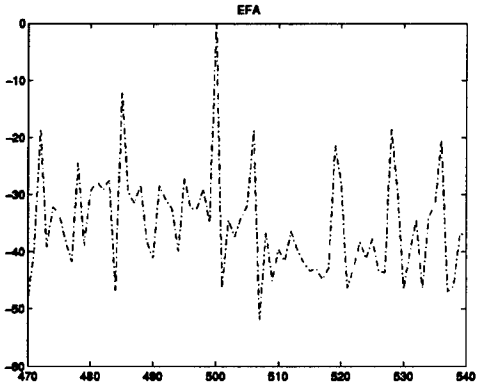


e) EFA

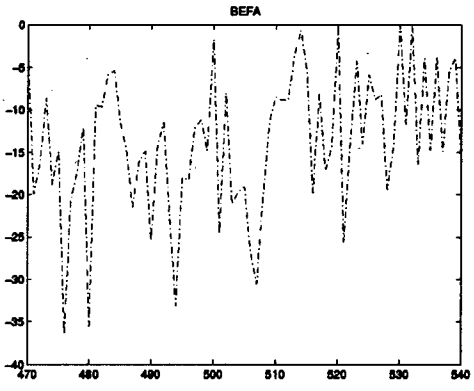


f) BEFA

**Figure 26)** Performance comparison when target is inserted at range 500, case a.

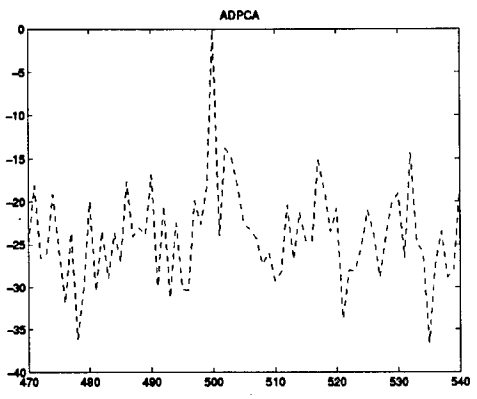


a) ADPCA

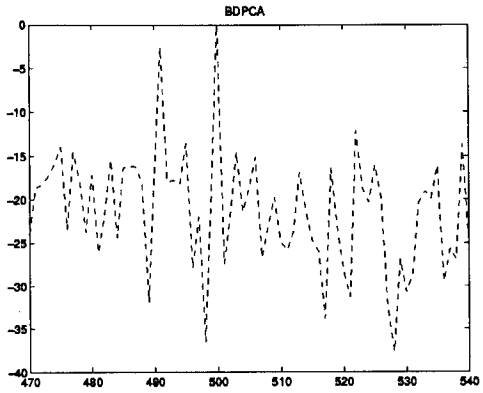


b) BDPCA

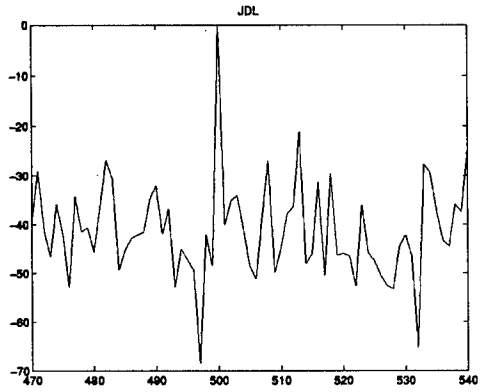


c) JDL

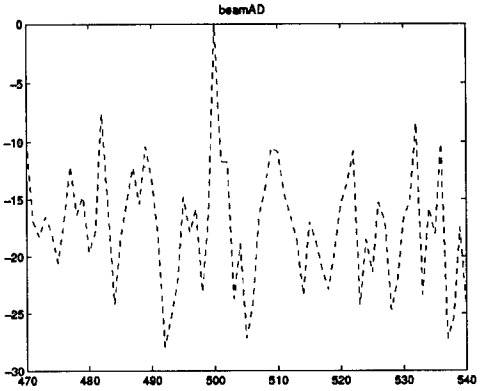


d) BeamAD

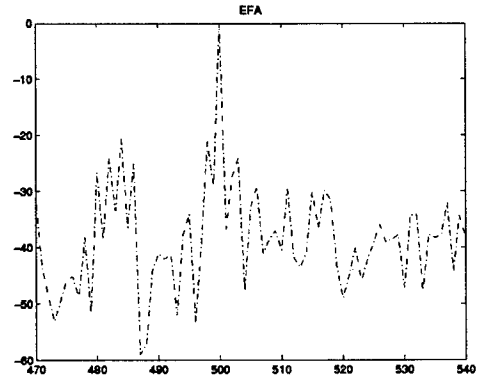


e) EFA

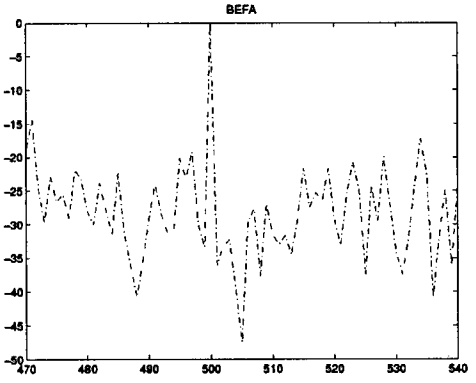


f) BEFA

**Figure 27)** Performance comparison when target is inserted at range 500, case b.

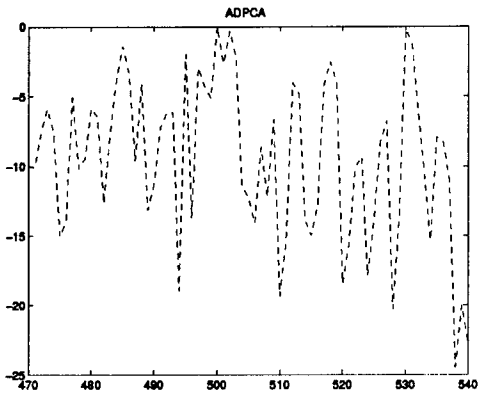


a) ADPCA

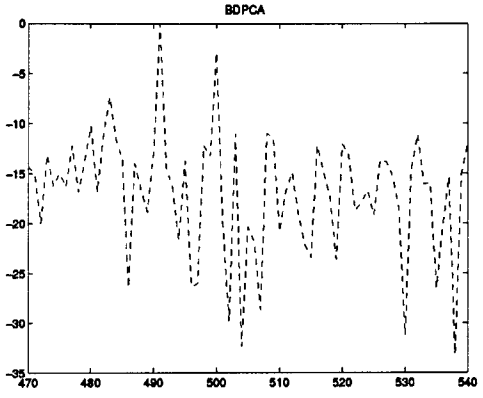


b) BDPCA

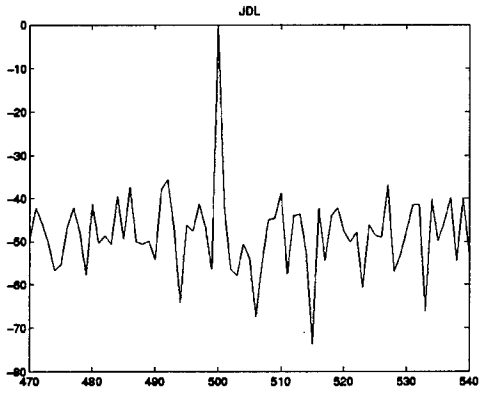


c) JDL

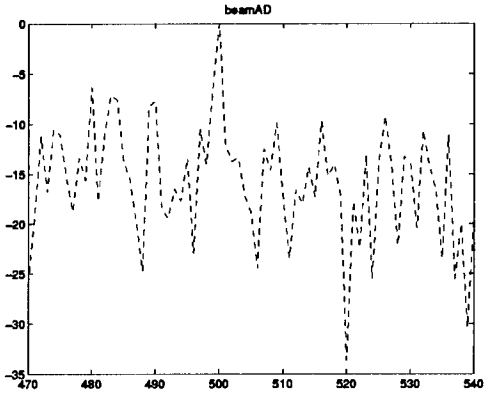


d) BeamAD

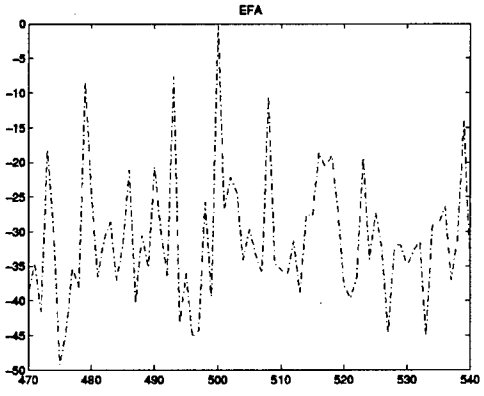


d) EFA

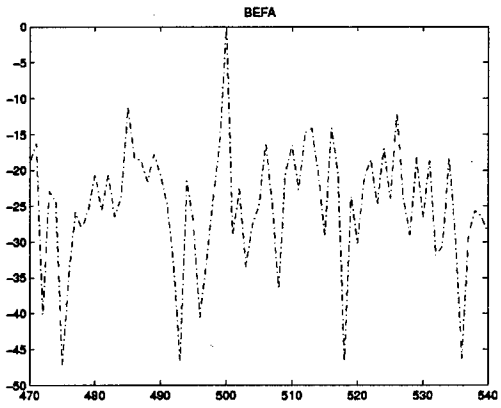


f) BEFA

**Figure 28)** Performance comparison when target is inserted at range 500, case c.

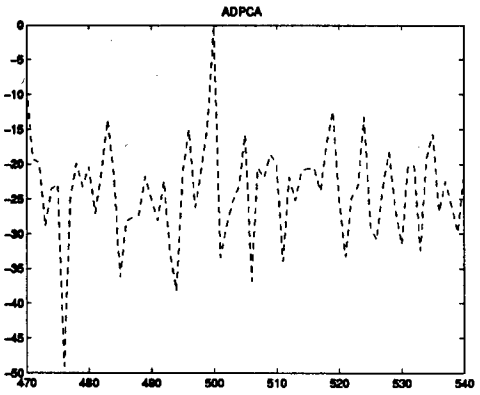


a) ADPCA

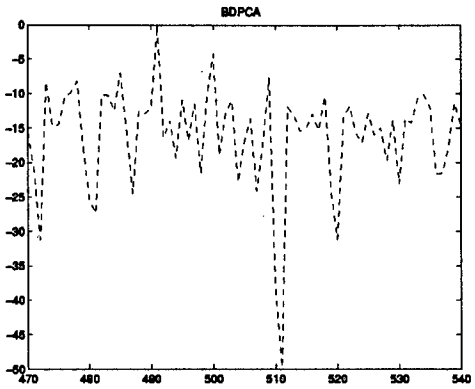


b) BDPCA

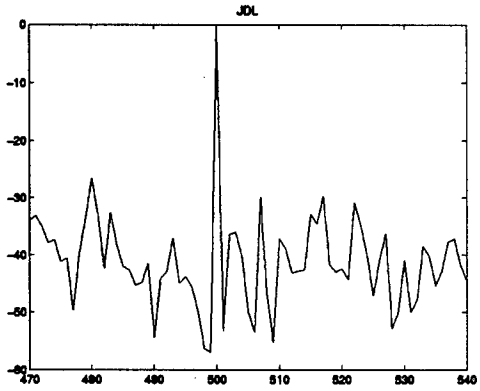


c) JDL

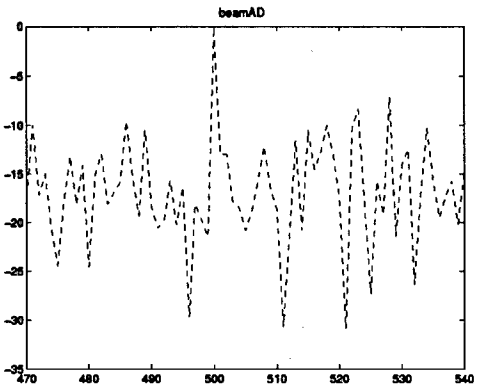


d) BeamAD

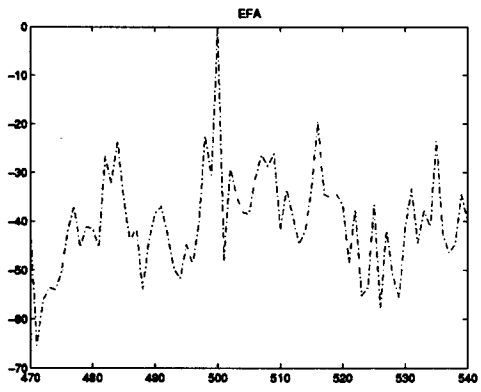


e) EFA

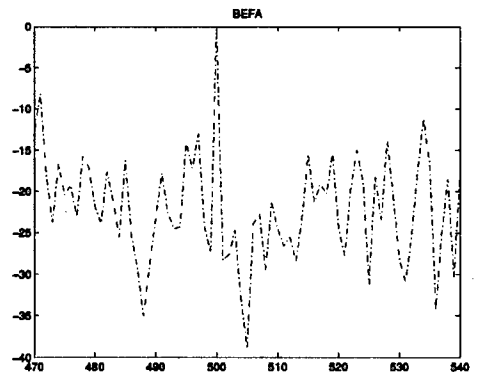


f) BEFA

**Figure 29)** Performance comparison when target is inserted at range 500, case d.

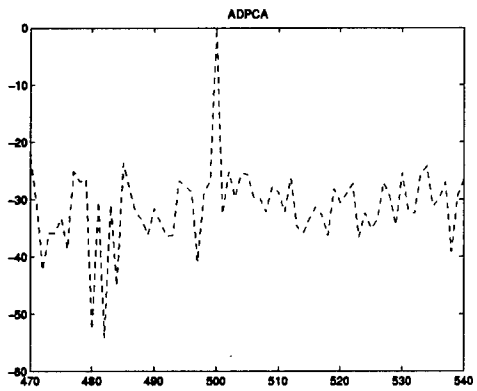


a) ADPCA

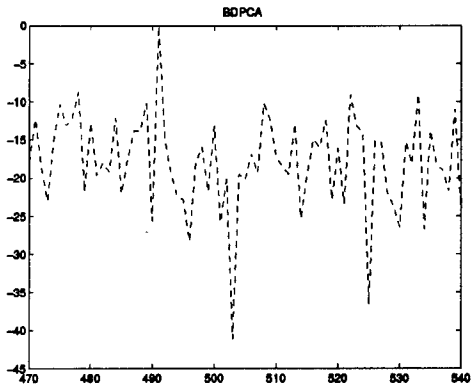


b) BDPCA

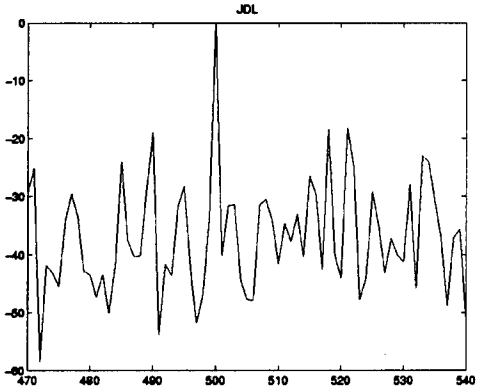


c) JDL

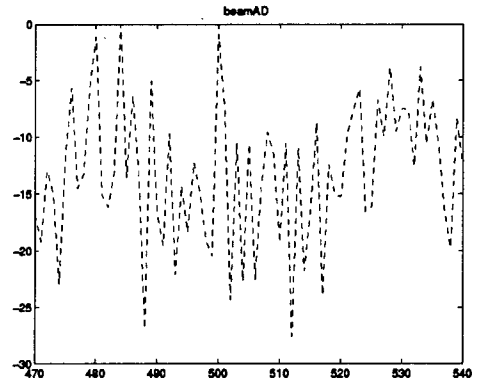


d) BeamAD

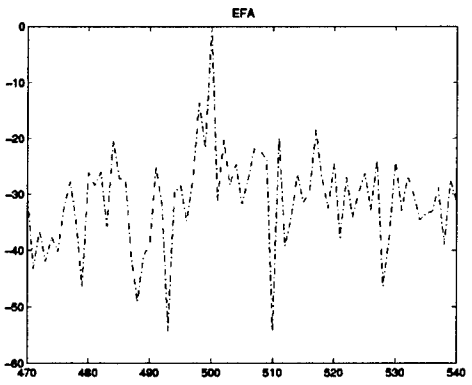


e) EFA

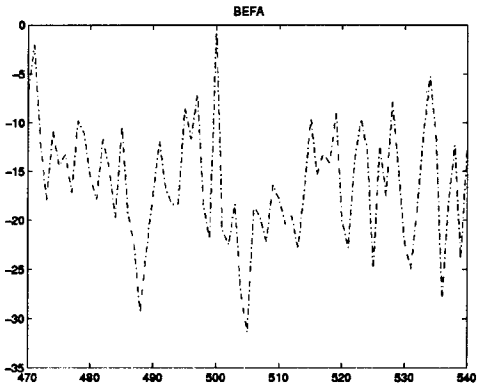


f) BEFA

**Figure 30)** Performance comparison when target is inserted at range 500, case e.

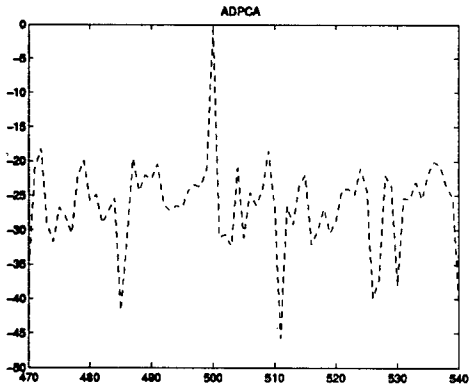


a) ADPCA

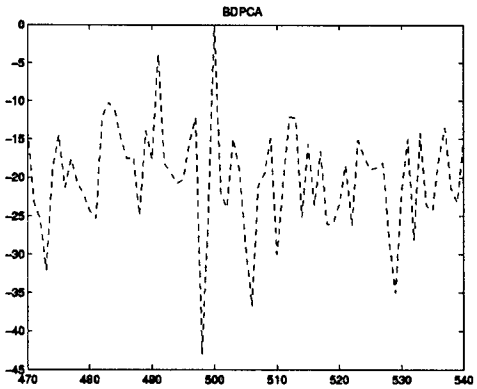


b) BDPCA

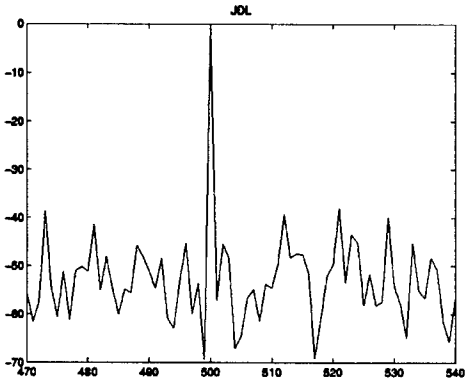


c) JDL

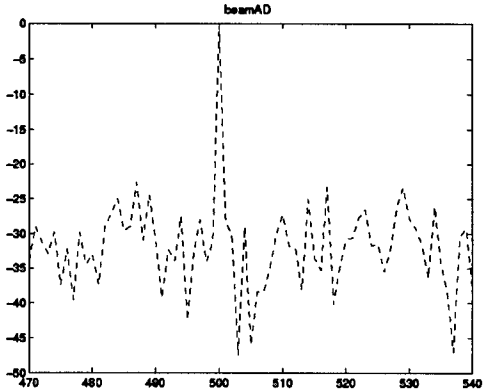


d) BeamAD

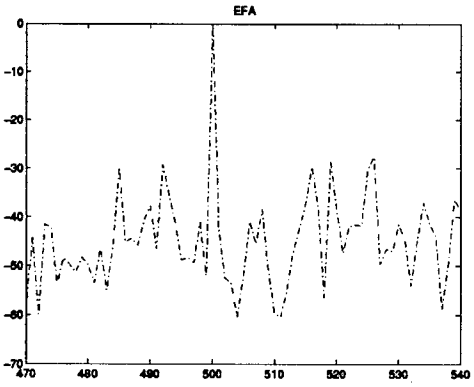


e) EFA

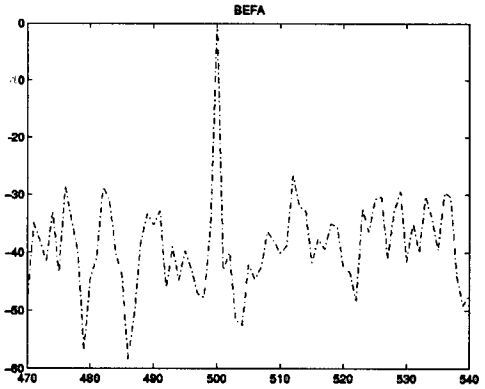


f) BEFA

**Figure 31)** Performance comparison when target is inserted at range 500, case f.

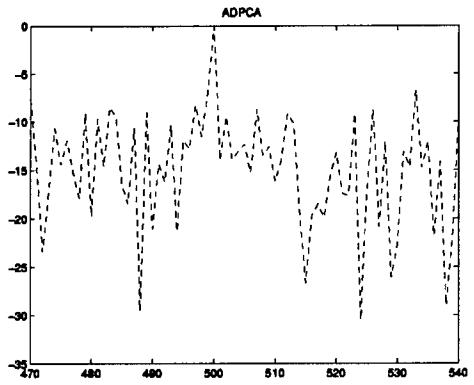


a) ADPCA

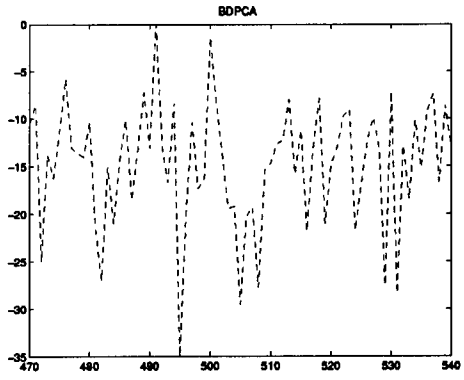


b) BDPCA

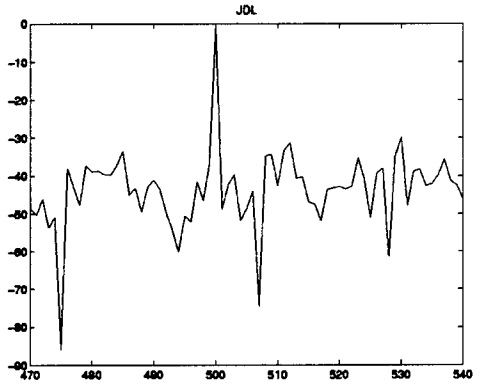


c) JDL

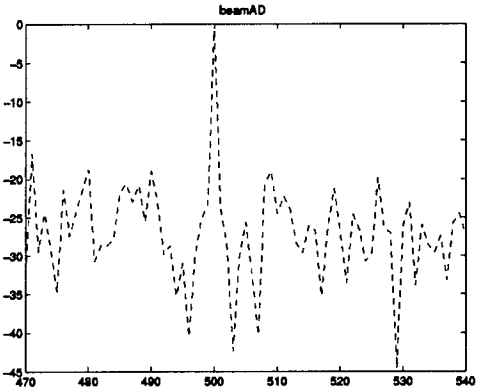


d) BeamAD

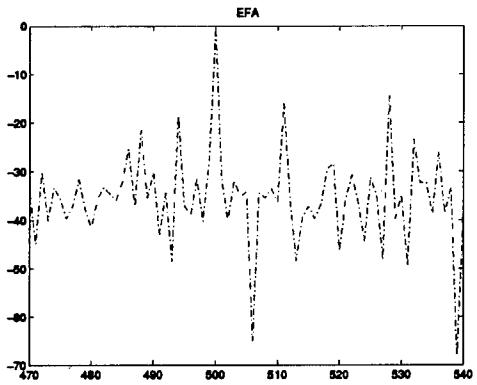


e) EFA

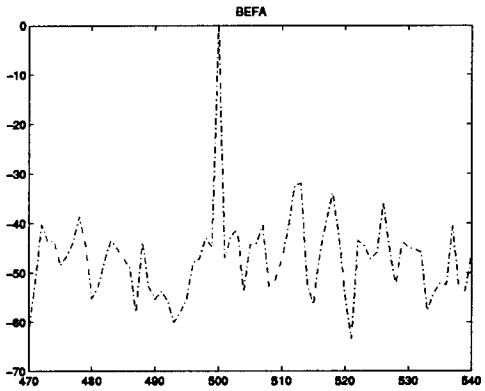


f) BEFA

**Figure 32)** Performance comparison when target is inserted at range 500, case g.

# APPENDIX 1

| Scheme | M | N | Kt | Ks | $A_p$ | G | Q |
|---|---|---|---|---|---|---|---|
| **ADPCA** | 128 | 22 | 3 | - | $[\ 0_{p\times 3},\ I_3,\ 0_{(125-p)\times 3}\ ]^T$ | $I_{22}$ | 66 |
| **EFA** | 128 | 22 | 3 | - | $[f_{128,Dp-1}, f_{128,Dp}, f_{128,Dp+1}]$ | $I_{22}$ | 66 |
| **FTS** | 128 | 22 | 1 | - | $f_{128,Dp}$ | $I_{22}$ | 22 |
| **Beamspace ADPCA** | 128 | 22 | 3 | 3 | $[\ 0_{p\times 3},\ I_3,\ 0_{(125-p)\times 3}\ ]^T$ | See Note | 10 |
| **Subarraying ADPCA** | 128 | 22 | 3 | 3 | $[\ 0_{p\times 3},\ I_3,\ 0_{(125-p)\times 3}\ ]^T$ | *G | 10 |
| **Subarraying EFA** | 128 | 22 | 3 | 3 | $[f_{128,Dp-1}, f_{128,Dp}, f_{128,Dp+1}]$ | * G | 10 |
| **Subarraying FTS** | 128 | 22 | 3 | 3 | $f_{128,Dp}$ | * G | 4 |
| **JDL** | 128 | 22 | 3 | 3 | $[f_{128,Dp-1}, f_{128,Dp}, f_{128,Dp+1}]$ | See Note | 10 |

Table 6) Parameters for comparison tests in this report.

Notes:

Q is used in (9), in this report.

**G** is the beamforming matrix which is formed as described in (13). When we use the uniform **g** vector, the **G** ($\mathbf{K_s}$=3 ) is as folows

$$G = \begin{bmatrix} 1 & 0 & 0 \\ 1 & 1 & 0 \\ 1 & 1 & 1 \\ 1 & 1 & 1 \\ 1 & 1 & 1 \\ 1 & 1 & 1 \\ 1 & 1 & 1 \\ 1 & 1 & 1 \\ 1 & 1 & 1 \\ 1 & 1 & 1 \\ 1 & 1 & 1 \\ 1 & 1 & 1 \\ 1 & 1 & 1 \\ 1 & 1 & 1 \\ 1 & 1 & 1 \\ 1 & 1 & 1 \\ 1 & 1 & 1 \\ 1 & 1 & 1 \\ 1 & 1 & 1 \\ 1 & 1 & 1 \\ 0 & 1 & 1 \\ 0 & 0 & 1 \end{bmatrix}$$

**Note:** MCARM data is not collected by a uniformly spaced linear antenna array, so its beamforming matrix is relatively complicated. This G matrix used in beamspace ADPCA and JDL can be obtained by using measured steering vector information provided with the MCARM database. See the discussion on modSA at [5].

# APPENDIX 2

For real data it is difficult to evaluate if there is a mismatch between the statistics for the reference data and the statistics for the data from the cell-under-test. However by considering energy fluctuations over range, it is possible to partially evaluate this. When the mismatch is near the target location, it could degrade the performance dramatically. To evaluate how stationary the reference data is and to determine how the statistics of the reference data and the statistics for the data from the cell-under-test are mismatched near the target, we plot energy fluctuations over 33 range cells on each side of the target. For each range we plot the average over 11 neighboring Doppler bins and 11 neighboring angle bins near the target Doppler and angle bin. We use 5 Doppler and angle bins on each side of the target. The results are given in Fig. 33 through Fig. 36.

In Fig. 33 through Fig. 36, in all plots the data seems to be non-stationary. But we judge that when the number and the duration of the humps and the nulls increases in these plots, the degree of non-stationary of the data also increases. Generally when the data is highly non-stationary the beamspace post-doppler schemes JDL and BEFA outperform EFA and the other element space schemes.

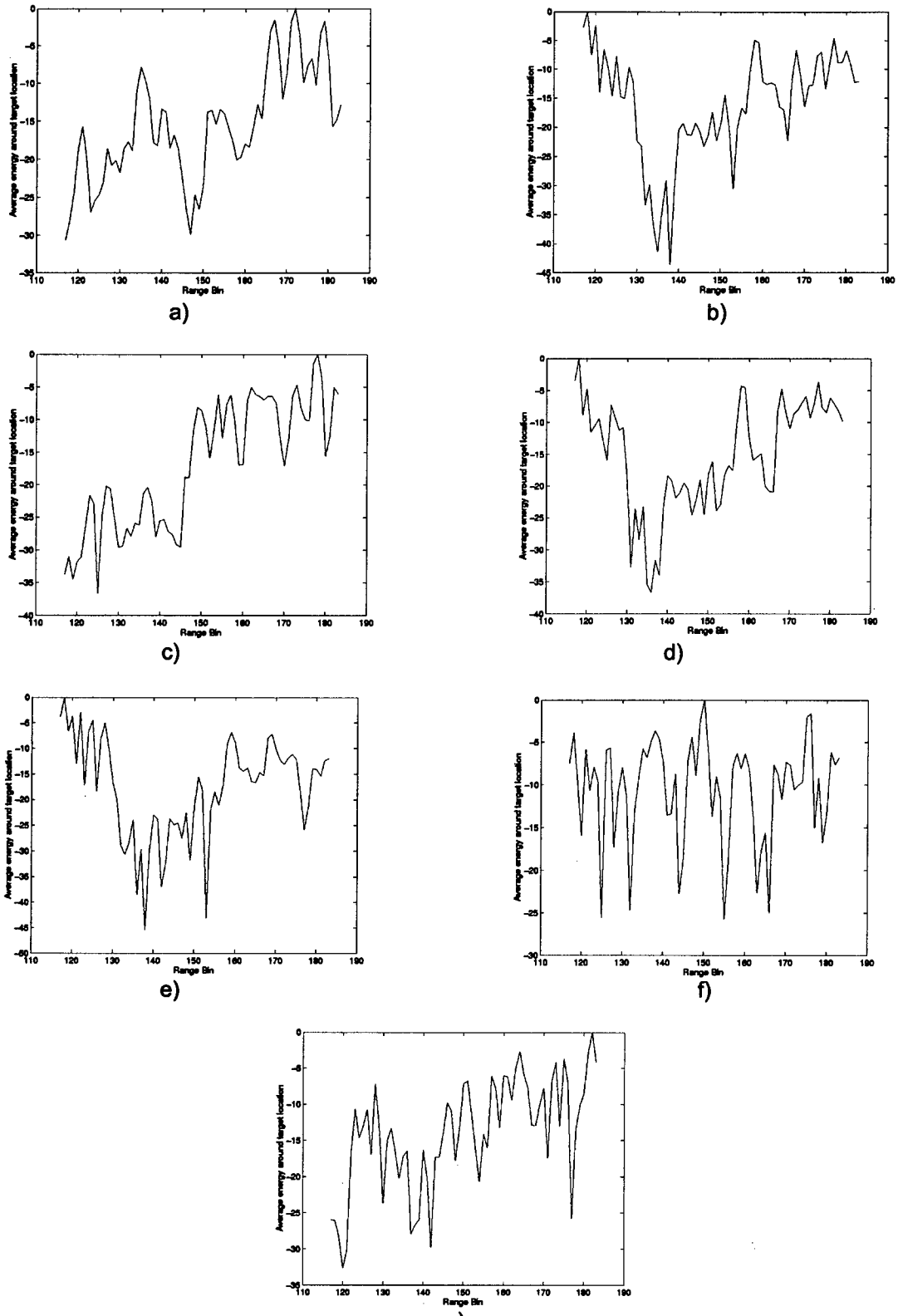


**Figure 33)** Energy plots for case a , b , c, d, e ,f ,g , when the target is located at range 150. (Example 1).

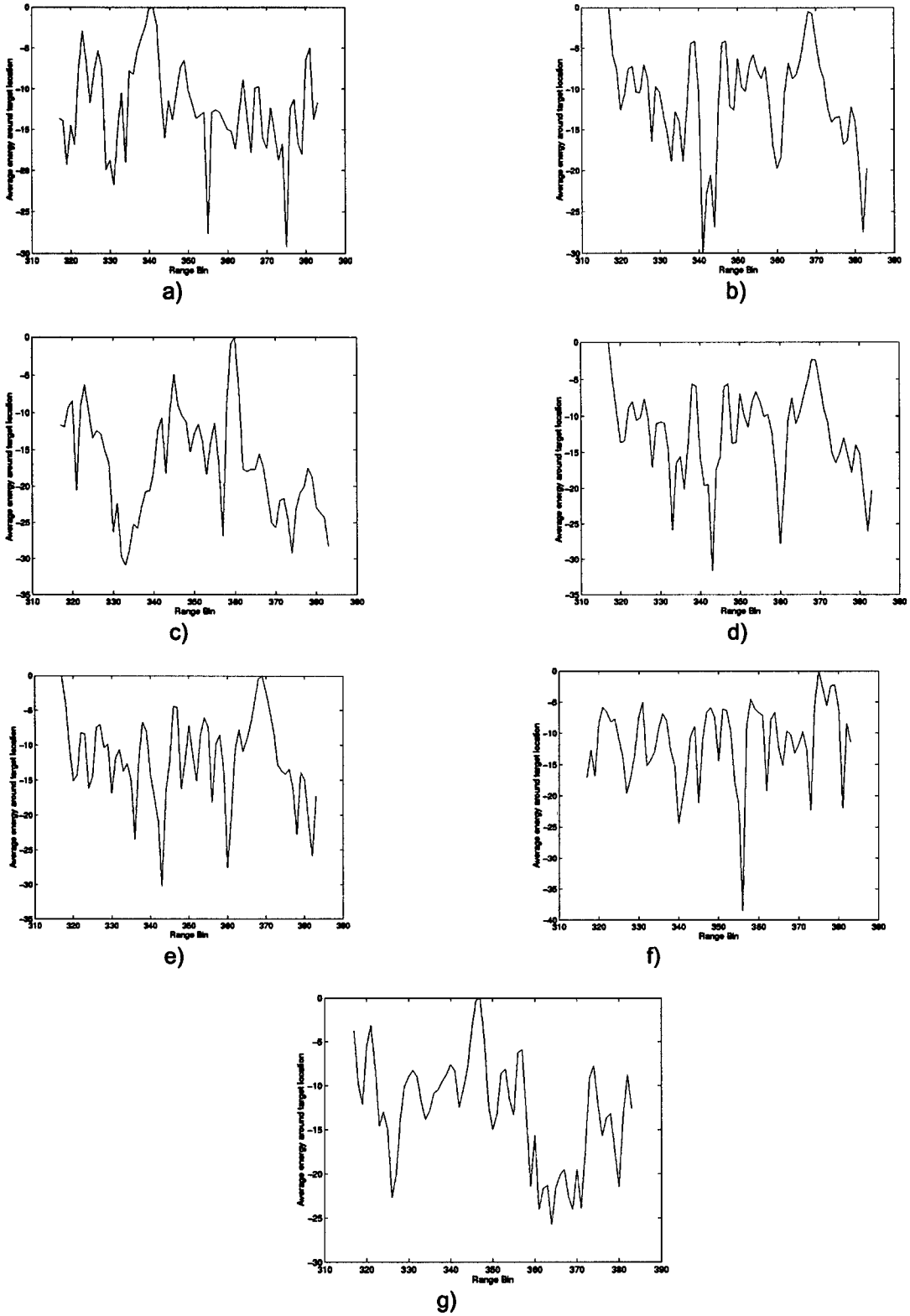


**Figure 34)** Energy plots for case a, b, c, d, e, f when the target is located at range 350. (Example 2).

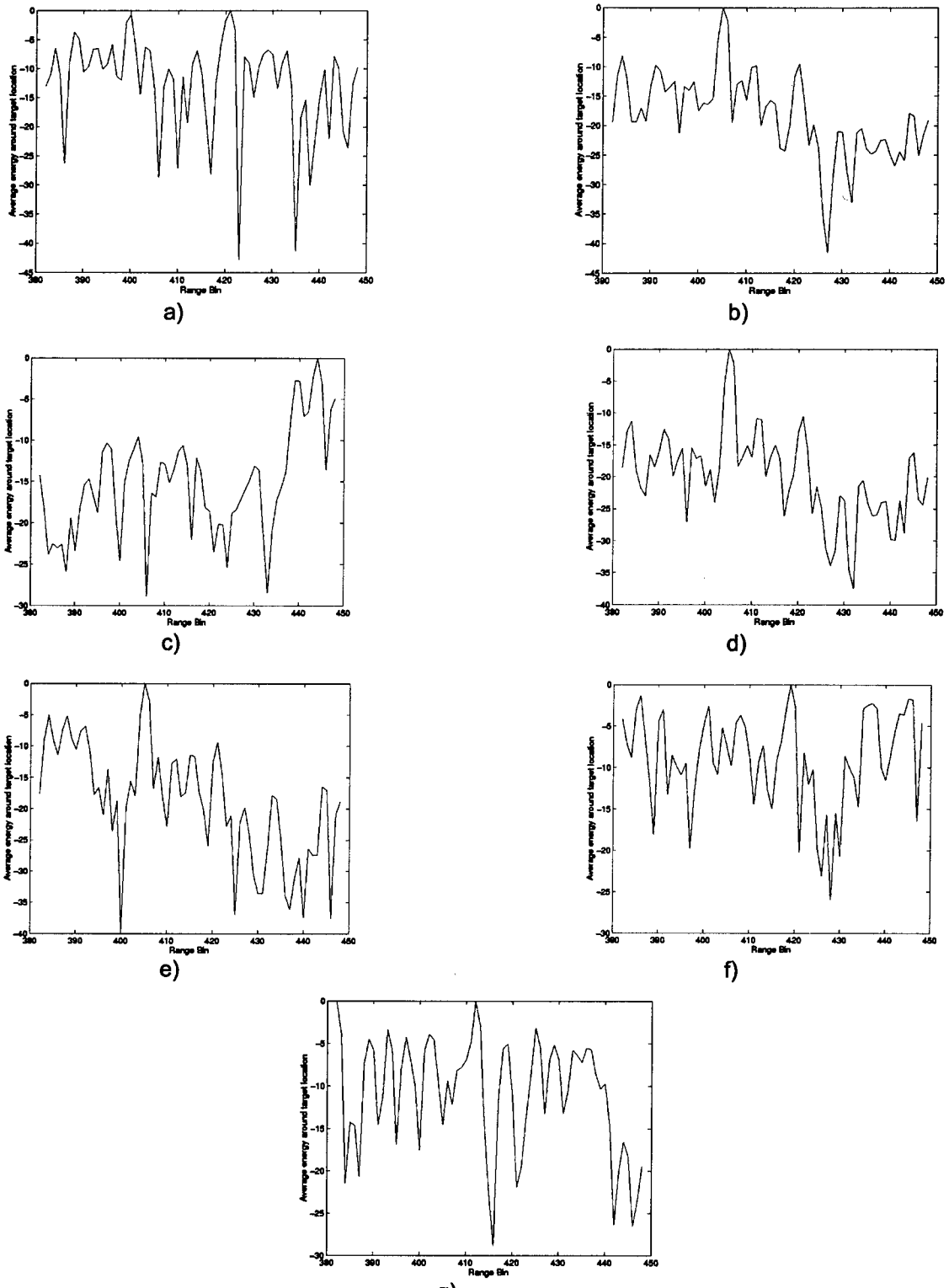


**Figure 35)** Energy plots for case a, b, c, d, e, f, g when the target is located at range 415. (Example 3).

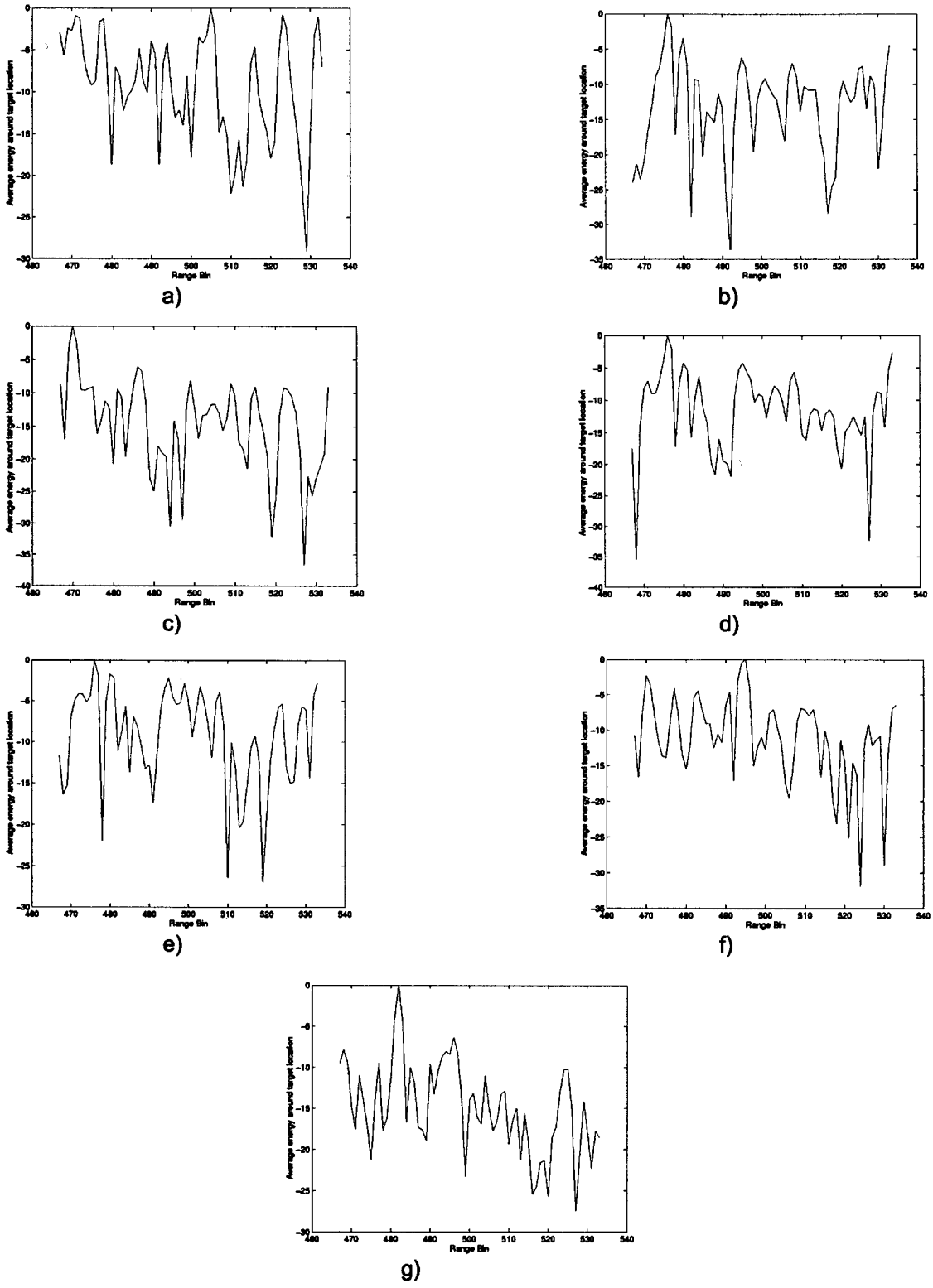


**Figure 36)** Energy plots for case a, b, c, d, e, f, g f when the target is located at range 500. (Example 4)

# 4. REFERENCES


1. J.Ward, *Space–Time Adaptive Processing for Airborne Radar*, Technical Report 1015, MIT Lincoln Laboratory, December, 1994.

2. Z. Gu, *Performance Comparison of STAP Schemes For Airborne Radar*, Masters Thesis, Lehigh University, December , 1996.

3. A. Oppenheim and R. Schafer, *Discrete-Time Signal processing*, Prentice Hall, Englewood Cliffs, New Jersey, 1989.

4. M. D. Zoltowski, "*Beamspace M.L. Bearing Estimation for Adaptive Phased Array Radar*", In Adaptive Radar Detection and Estimation, S. Haykin and A. Steinhardt Editors, John Wiley and Sons, New York, 1992.

5. MCARM database web site, Rome Laboratory USAF, 'http://128.132.2.229'

* 6. D. Sloper et al., *MCARM Final Report*, Rome Lab Tech. Rept., RL-TR-96-49, April 1996.

7. L W. Melvin and B. Himed, "Comparative Analysis of Space –Time Adaptive Algorithms with Measured Airborne Data", *presented at the 7th International Conference on Signal Processing Applications and Technology*, October 7-10, 1996 .

8. W. Melvin, H.Wang and M. Wicks, "*Multichannel Airborne Radar Array Data Analysis*", presented at 41st Annual Tri-Service radar symposium, June 1995.

9. H. Wang, "*Space-Time Processing and Its Radar Applications*", notes used for the class ELE 891 at Syracuse University, Summer 1995.


*Although this report references the above limited report, no limited information has been extracted.

*U.S. GOVERNMENT PRINTING OFFICE: 2001-610-055-10062